Chapter in "Alloy Design,"
John K. Tien and George S.
Ansell, editors, Academic Press

LBL-2782
Preprint c.2 Repl.

ALLOY DESIGN FOR FRACTURE TOUGHNESS

V. F. Zackay and E. R. Parker

June 1974

Prepared for the U. S. Atomic Energy Commission
under Contract W-7405-ENG-48

TWO-WEEK LOAN COPY

This is a Library Circulating Copy which may be borrowed for two weeks. For a personal retention copy, call Tech. Info. Division, Ext. 5545

LAWRENCE BERKELEY LABORATORY
UNIVERSITY OF CALIFORNIA
BERKELEY

LBL-2782 c.2 Repl.

DISCLAIMER

This document was prepared as an account of work sponsored by the United States Government. While this document is believed to contain correct information, neither the United States Government nor any agency thereof, nor the Regents of the University of California, nor any of their employees, makes any warranty, express or implied, or assumes any legal responsibility for the accuracy, completeness, or usefulness of any information, apparatus, product, or process disclosed, or represents that its use would not infringe privately owned rights. Reference herein to any specific commercial product, process, or service by its trade name, trademark, manufacturer, or otherwise, does not necessarily constitute or imply its endorsement, recommendation, or favoring by the United States Government or any agency thereof, or the Regents of the University of California. The views and opinions of authors expressed herein do not necessarily state or reflect those of the United States Government or any agency thereof or the Regents of the University of California.

TABLE OF CONTENTS

INTRODUCTION..... 1

DISCUSSION..... 2

I. Historical Perspective..... 2 - 8

II. Designing for Toughness..... 8 - 30

A. The Transition Temperature Approach..... 8 - 11

B. The Fracture Mechanics Approach..... 11 - 28

C. An Important Unsolved Problem..... 28 - 30

ACKNOWLEDGMENTS..... 30

REFERENCES..... 31 - 36

TABLES..... 37 - 39

FIGURE CAPTIONS..... 40 - 42

ALLOY DESIGN FOR FRACTURE TOUGHNESS

by

V. F. Zackay and E. R. Parker

Center for the Design of Alloys, Inorganic Materials Research Division, Lawrence Berkeley Laboratory and Department of Materials Science and Engineering, College of Engineering; University of California, Berkeley, California 94720

INTRODUCTION:

The most important mechanical property required of a structural material is resistance to sudden or catastrophic fracture. For this reason, metals are usually the materials of choice where such failure would result in loss of life or property. The resistance of metals to catastrophic failure is, however, not an intrinsic and fixed quantity. On the contrary, it changes with the amount and type of stress, the temperature, the strain rate, and environmental variables, i.e., macroscopic factors, as well as with alloy composition and structure, i.e., microscopic factors. Consideration of only one set of these factors in either the design of an engineering structure or, alternatively, in the design of an alloy is inconsistent in principle and ineffective in practice.

This review describes some of the progress made in both the macroscopic and microscopic approaches to the problem of designing alloys with superior fracture toughness. Following a brief review of the striking progress made in the past ten years in the macroscopic field of continuum mechanics, the influence of the microscopic variables of composition, defect structure, and microstructure are considered. Illustrative examples are taken from the authors' own research and from the literature.

DISCUSSION

I. Historical Perspective

In a review of a field as active and varied as the fracture toughness of metals, historical perspective can be helpful. A simple but reliable way of obtaining perspective is to peruse the published proceedings of the national and international fracture conferences that have been held every five to ten years since 1950.

A conference on the fatigue and fracture of metals was held at the Massachusetts Institute of Technology in June, 1950. The papers on fracture toughness presented at this conference can be conveniently grouped into the two categories mentioned previously, viz., macroscopic and microscopic. Several papers having the macroscopic viewpoint were concerned with interpretating brittle failures in large structures such as ships and planes. These interpretations were made with the aid of classical engineering stress analysis and were concerned with design criteria such as the presence and configuration of notches, faulty workmanship encountered in welding practices, and evaluations of the quality of the steel by macroscopic observations of fracture surfaces. In other papers with the macroscopic viewpoint, the tendency for brittle fracture in steel, measured by either the Charpy, notched tensile or slow bend test, was discussed in terms of the shift of the ductile-brittle transition temperature. The influence of test variables such as temperature, strain rate, notch acuity, and composition was recognized but was difficult to reconcile into a unified theory. The variation of transition temperature with type of specimen and nature of test obviously posed great difficulties

in analysis to the conference attendees. It is of interest to note that one paper in the microscopic category, given by Orowan, is now regarded as a historical milestone in the development of a quantitative theory of fracture toughness. Orowan suggested that the surface energy term, γ, in the Griffith theory of fracture as applied to metals, be substituted by a term, E_p, which symbolized the energy absorbed by microscopic plastic flow in front of the moving crack. Lastly, the conferees were well aware of the importance of the role played by microstructure in temper embrittlement and in fatigue failures, but their knowledge of defect structure and microstructure was limited by the low resolution of the available instrumentation for the characterization and identification of structure.

The international conference on fracture held in Swampscott, Massachusetts in April, 1959, must be considered a major event in the progress toward a comprehensive treatment of the fracture of solids. Although less than a decade had passed since the 1950 conference, tremendous advances had been made in the understanding of the atomistic and microstructural features of fracture in metallic, ceramic and polymeric materials. So much significant progress was reported at this conference that it is difficult to select the most important advance. It was, however, abundantly clear that one outstanding achievement was the application of dislocation theory to both the theoretical and experimental aspects of fracture. Further, the importance of microstructural features such as slip bands, twins, grain boundaries, and brittle phases was qualitatively delineated in metals and in some ceramics for fracture under static, dynamic, and cyclic types of loading at both room and elevated temperatures. One prominent feature of the conference was the reported use of new high

resolution tools such as the electron microscope to characterize the interior structure and the fracture surface morphology (by replication techniques).

The sessions on cleavage fracture, ductile fracture and fatigue, and elevated temperature fracture were summarized by Barrett, Honeycombe, and Grant, respectively. They restated some of the pivotal unanswered questions raised during the conference. Conferees agreed that the Griffith equation was satisfactory as a first approximation (in its modified form) but questioned whether it could be made more quantitative or that it would ever be capable of predicting the effect of variables such as temperature and strain rate on the fracture of solids. Another conference question related to the disproportionate emphasis on the fracture behavior of relatively simple materials, i.e., single and bicrystals of pure metals. Relatively little understanding had been gained with respect to the fracture of the more complex materials of engineering structures. Last, and perhaps most significant, relatively little had been accomplished to reconcile the atomic and microscopic views of fracture with the macroscopic ones of mathematical plasticity --- an essential linkage if new and superior engineering materials were to be developed from the first principles of materials science. It is interesting --- and satisfying --- that all of these questions were partially or completely answered within the next decade.

In the ensuing fifteen years, there were many national and international conferences on the subject of fracture, as well as several new journals and many new books. The topic of fracture, always intensely interesting to scientists and engineers for obvious reasons, has become

one of the most popular areas of research in physical metallurgy. Why is this so? What has happened to bring about this explosion of interest? Clues to the answers to these questions are found in the questions raised at Swampscott. As mentioned previously, the conferees at Swampscott had difficulty, in spite of their successes, in reconciling the atomistic and microstructural views of fracture as enunciated primarily by materials scientists, with those of macroscopic mathematical plasticity as promulgated largely by engineers. This difficulty was also reflected in the type of materials that were being studied, viz., most of the experimental effort was on single crystals and/or high purity metals instead of the complex alloys used in engineering structures.

A series of papers by Irwin and his colleagues in the late 1950s and early 1960s dramatically solved these problems. This pioneering work introduced concepts which have led to significant progress in the unification of the microscopic and macroscopic views of fracture. Perhaps most significant of all, the practical application of these concepts has already proven effective in reducing the possibility of catastrophic fracture in engineering structures.

The original data of Irwin and his colleagues were expressed in terms of the critical value of the strain (or potential) energy release rate G_C, at which unstable crack propagation occurred. Irwin's basic approach was, therefore, analogous to Griffith's, viz., a thermodynamic one. Irwin's approach provided a convenient parameter to include all supplementary energy-dissipating terms, such as plastic flow, which could in turn produce heat or sound, in addition to the work required to fracture the lattice. The constancy of G_C, and hence its use as a

measure of the resistance of a material to fracture depends critically on experimental testing conditions, but for situations where plastic flow preceding crack extension is small and localized within a small area, the critical value can always be related to the failure stress using linear elastic methods. Irwin's parameter, G_C, became known as "fracture toughness," although this term is now generally reserved for the associated value of critical stress intensity, K_C.

The disadvantage of using the critical strain energy release rate, G_C, is that fracture is considered, although indirectly, in terms of a complex energy concept. This difficulty is removed if fracture is considered in terms of the elastic stress components adjacent to the crack tip. Westergard showed that the stress σ_y in the direction normal to the plane of the crack, and at a point (on the crack plane) distant "r" from the crack tip, reduced to the following expression:

$$\sigma_y = K\sqrt{2\pi r}$$

where K is the stress intensity factor. For elastic loading the strain energy is uniquely defined by the stress distribution. Thus, a simple relationship exists between the stress intensity factor K and the strain energy release rate G. For plane stress, $K_C^2 = G_C E$ while for plane strain, $K_{IC}^2 = \frac{G_{IC}E}{1 - \nu^2}$ where ν is Poissons ratio and E is Young's modulus of elasticity.

The only section of fracture mechanics which has so far been rigorously formulated is that of linear elastic fracture mechanics although much progress is being made in non-linear concepts such as the "J-integral" approach. Thus, at present, fracture mechanics can be used only for

elastic brittle materials or materials which approach this limit. Examples are high strength aluminum alloys, glass, high strength steel (the fracture characteristics of these materials are relatively insensitive to temperature and strain rate) and the propagation, but not the initiation, of a crack in low strength steel under cyclic loading. Thus, designing against brittle fracture requires two approaches, one for strain rate- and temperature-sensitive materials --- the transition temperature approach --- and the other for strain rate- and temperature-insensitive materials --- the fracture mechanics approach.

Both the above-mentioned approaches have been discussed in detail in the recent literature. Some representative reviews are given below. Tetelman and McEvily (1967), in their book entitled, "Fracture of Structural Materials," comprehensively discuss both the transition temperature and the fracture mechanics approaches. The relative roles of composition and microstructure are treated in both these approaches. Knott (1973), in a recent monograph entitled, "Fundamentals of Fracture Mechanics," concisely and rigorously develops the historical evolution of fracture mechanics in a manner useful to both the designer and the physical metallurgist.

In a provocative study, Averbach (1968) derives quantitative relationships between the macroscopic and the microscopic variables of fracture of simple solids. Pellini and his coworkers have been pioneers in the transition temperature aspect of fracture. Recent papers by Pellini (1968), Puzak and Lange (1969), and Loss and Pellini (1969) are representative of their work. For a detailed and comprehensive review of the whole

field of fracture the series of volumes edited by Liebowitz (1968) is invaluable. Lastly, the Proceedings of the Second Tewksbury Symposium, edited by Osborn et al. (1969) is a thoughtful review of the progress made in applying what is currently known about fracture to the design of useful engineering structures. Much of the foregoing discussion was based on the review papers of this symposium and on the discussion of the evolution of modern fracture mechanics by Knott (1973).

II. Designing for Toughness

In the ensuing discussion, examples of both the transition temperature and the fracture mechanics approaches to the design against brittle fracture are presented. The relationships between the macroscopic and microscopic viewpoints are stressed. In each case, the objective was to achieve, through compositional and microstructural control, improved combinations of strength, ductility and toughness.

A. The Transition Temperature Approach

Metals or alloys with the bcc structure can fail either by shear or by cleavage. It is now well established that the propensity of bcc metals to fail by cleavage is influenced by a host of compositional and structural variables. The temperature of transition from a high energy shear fracture to a low-energy cleavage fracture, for a given type of test, is a convenient measure of the influence of these variables. Some of the compositional and structural variables known to decrease the transition temperature in bcc iron-base alloys are: (1) the lowest possible level of interstitials in solid solution (interstitials raise the critical resolved shear stress of bcc metals to the cleavage stress as the temperature is lowered), (2) the maximum amounts of either nickel

or manganese in solid solution commensurate with other metallurgical considerations, and (3) the finest possible grain size. This listing of desirable features is, of course, not complete and is intended only as a guide for the selection of an alloy system for study. The system Fe-Ni-Ti appears to be particularly appropriate for such a study. The titanium and nickel contents in these alloys can be varied to meet requirements (1) and (2) above. Fine grain sizes can be obtained by thermal or thermal-mechanical means. In the investigation summarized in the following discussion the nickel content was varied from 8 to 16% while the titanium content was kept constant at 0.5%. Details of this and related work are given in the papers by Horwood (1972), Sasaki (1973), Zackay (1973), Jin et al. (1973 a,b,c), Yokota et al. (1974 a,b), and Sasaki et al. (1974).

The change in the impact toughness at -196°C of specimens of an Fe-12% Ni-0.5%Ti alloys as a function of thermal and thermal-mechanical history is summarized in Fig. 1. All specimens were given a 900°C solution treatment and then reheated to the temperatures indicated prior to testing at -196°C. The range of reheat temperatures included the lower and upper limits of temperature of the two phase ($\alpha+\gamma$) region (shown by the horizontal broken lines in the figure) as well as the lower part of the single phase (γ) region. The Charpy impact energies showed a gradual increase with reheat temperature in the upper limit of the two phase ($\alpha+\gamma$) region. Abrupt increases in impact energy were observed when the reheat temperatures were inside of a one hundred degree range which was above the lower limit of the single phase (γ) region, as

shown by curve A. Reheat temperatures above this range, however, resulted in a sharp decline in impact toughness, as shown in the figure. All specimens exhibiting the peak Charpy values were characterized by microstructures having a fine grain size, while those with low values were coarse grained. Electron microscope examination by replication techniques suggested that new grains formed at prior austenitic and martensite lath colony boundaries via dissolution of the two phase ($\alpha + \gamma$) duplex structure which had formed on heating.

Substantiation of this apparent grain refining mechanism was obtained by systematically varying the thermal history of specimens. Specimens were first heated to 650°C prior to raising the reheat temperature to between 750-800°C. This initial low temperature treatment resulted in broadening the reheating temperature vs. Charpy energy curve as shown in Fig. 1, curve B. The microstructures of specimens within the peak region delineated by curve B were, as expected, single phase and fine grained. A similar improvement in toughness and associated microstructures was produced by a process essentially equivalent to that described above, viz., by slowly heating the specimens through the two phase ($\alpha + \gamma$) region on the way up to the higher temperatures. Cold working prior to reheating produced an even finer grain size at the reheating temperatures investigated. The Charpy energy as a function of reheating temperature for the cold worked specimens is shown in Fig. 1, curve C.

The relationship between the refined prior austenite grain size and the resulting impact toughness is given in Fig. 2, in which the impact energy at -196°C is plotted vs. the grain size for the several grain refining treatments described above. The results showed that regardless

of the grain refining method used, there was a sharp drop in impact energy above a critical grain size of about 15 microns. Similar relationships existed for all the alloys investigated. For the 8% Ni alloy, the critical grain size was about 5 microns, and for the 16% Ni alloy, about 30 microns.

Studies of the type described above established useful relationships between nickel content, grain size and impact toughness for a family of nickel-containing and titanium-stabilized alloys. Practical implementation of these studies could eventually result in the design of cryogenic steels with desirable combinations of strength, ductility, and toughness.

B. The Fracture Mechanics Approach

1. Metastable Austenitic Steels

The mechanical properties of steels with a metastable austenitic matrix are known to be highly dependent on the composition, the temperature of testing, the state of stress, the prior history of processing, and the strain rate (Bhandarkar et al., 1972). In some alloy systems a phase transformation may be initiated by elastic or plastic deformation. Some commercial stainless steels (AISI Type 300 series) undergo an austenite to martensite phase transformation when deformed. However, these commercially available steels have relatively low yield strengths. In a recent development, deformation induced phase transformations were utilized to create a new class of ultra-high strength metastable austenitic steels, known as TRIP steels (Zackay et al., 1967). (The word TRIP is an acronym of transformation induced plasticity.) The alloy content of TRIP steels is adjusted so that the face centered cubic phase is thermally stable at room temperature. When these alloys are deformed, they transform

to the body centered martensitic phase, and fracture is attended by a considerable amount of plastic deformation even at high strength levels. Both the plastic deformation and the transformation enhance energy absorption at the tip of a moving crack and result in a higher critical energy release rate (G_{IC}) for crack propagation. This suggests that a fracture mechanics approach can be fruitful in designing high strength TRIP steels with high toughness.

The fraction of the volume that transforms for each unit of strain depends upon austenite stability, which in turn is determined by the composition, the prior history, the test temperature, and the test strain rate. The uniform elongation, rate of work hardening, yield strength, ultimate tensile strength, and fracture toughness are all strongly influenced by the stability of the austenite, as is shown in detail in a later section.

In a recent study, Bhandarkar et al. (1972) determined the influences of composition, processing conditions, and test temperature on the stability of austenite. Parts of the following discussion are based upon the results of their study. The chemical compositions of several of the steels involved are given in Table I. All the alloys listed were deformed 70% at a temperature of 450°C, unless otherwise designated. The primary purpose of such prior deformation of the austenite in TRIP steels is to raise the yield strength, often to 200,000 psi or more.

It is possible to obtain experimentally an austenite stability index for TRIP steels. With this index, predictions can be made of the effect of composition and processing conditions on mechanical

properties. Gerberich et al. (1970) have suggested that the volume fraction of martensite, V_α, produced during a tensile test varies as

$$V_\alpha = m\varepsilon^{\frac{1}{2}}$$

where m is a constant for a given set of test conditions and ε is the conventional strain. The transformation coefficient, m, was found to be a useful index of austenite stability, with higher values of m indicating lower degrees of stability. The value of m is readily obtained by plotting V_α vs. $\varepsilon^{\frac{1}{2}}$ and fitting the best straight line to the plot. Typical experimental data for steel CN8Cr are shown in Fig. 3 for a test temperature of -78°C. In TRIP steels the coefficient m can be varied from zero (completely stable) to about 3.5 (highly unstable). The value of m is zero when the test temperature is at or above the M_d temperature --- the temperature above which plastic strain will not induce a transformation. Another phase transformation temperature of importance in these steels is the M_s, which is the temperature at which martensite starts to form in an unstressed steel during cooling. The M_s is always below the M_d. TRIP steels are designed to be used at service temperatures between the M_s and M_d. In this temperature range, the austenite is thermally stable with respect to the service temperature but unstable with respect to strain. At temperatures well below the M_d and close to the M_s, the steel becomes so unstable that even an elastic deformation can induce a transformation (Scheil, 1932; Kulin et al., 1952; Angel, 1954; Fahr, 1969 and 1971; and Bhandarkar et al., 1972).

Bhandarkar et al. (1972) demonstrated the relationships between stability and mechanical properties for steels with stabilities varied by changes in test temperature (22° to -196°C), composition, (8, 12, 16, and 21% of Ni) and the prior deformation temperature (25° to 450°C). Examples of their results are shown in Figs. 4 and 5.

The engineering stress-strain curves at 22°C and -78°C are shown in Fig. 4 for the CN8Cr steel (composition given in Table I) deformed 70% at 450°C. The m values are also shown in the figure. The stress-strain curve obtained at 22°C exhibited a well-defined Lüders strain of about 6%, a low strain hardening rate, and an elongation of 20%; the m value was 1.85. The relatively low rate of strain hardening was a consequence of the comparatively low rate of martensite formation with strain. At a test temperature of -78°C, the stress-strain curve was quite different. The yield strength was lower by about 60,000 psi than that at 22°C, the Lüders strain was smaller and less well defined, the rate of strain hardening was much higher, and the elongation was about one-half of the room temperature value. These features are a consequence of the change in the stability produced by the temperature change (as reflected by the m value). Of particular interest are the low yield strength and the high rate of strain hardening. These features are characteristic of an alloy undergoing a stress induced phase transformation. At a strain of only 0.02, about half the austenite had already transformed to martensite in the -78°C test, as shown in Fig. 3. In the specimen tested at 22°C, less than 10% of the austenite had transformed at the same strain.

The stability can also be altered by changing the chemical composition or the prior deformation temperature. The stress-strain curves for three steels of different nickel contents, deformed 70% at 450°C and tested at -78°C, are shown in Fig. 5 (Bhandarkar et al., 1972). The striking difference between the curves is worthy of note. As Bressanelli and Moskowitz (1966), Gerberich et al. (1970), and Tamura et al. (1970) have observed, maximum elongation results when martensite is produced at an optimum rate with strain. Too little martensite forming per unit of strain results in early necking and too much causes premature failure. The relatively low m value for steel CN12Cr (estimated to be between 1.0 and 1.5) indicates that the criterion of an optimum m value for a large elongation has been met.

Changes in stability markedly influence the shape of stress-strain curves because Lüders strain, strain hardening rate, and elongation to fracture are affected by stability changes. In Fig. 6 are shown plots relating the stability coefficient, m, with elongation to fracture (Fig. 6(a)) and Lüders strain (Fig. 6(b)) for a large group of alloys of widely varying composition, processing histories, and testing temperatures (Gerberich et al., 1970).

Several investigators have suggested that a stress or strain induced phase transformation might enhance the absorption of energy and thereby increase fracture toughness (Gerberich et al., 1968, 1969, and 1971; Antolovich, 1968; Gerberich and Birat, 1971; and Antolovich and Singh, 1971). The fracture toughness of TRIP steels has been studied from both the theoretical and experimental viewpoints. It is clear from these studies that the toughness is dependent upon the stability, the chemical composition

of the strain induced martensite, and the strain rate. Gerberich et al. (1971) have shown that, as a first approximation, the fracture toughness K_C, is proportional to $m^{\frac{1}{2}}$. Room temperature plane stress fracture toughness values of almost 500,000 psi-$in^{\frac{1}{2}}$ were reported for highly unstable (m = 2) steels having yield strengths of 200,000 psi or higher; a summary of the data is shown in Fig. 7. The fracture toughness is decreased with increasing amounts of carbon plus nitrogen in an alloy. The effect of carbon and nitrogen contents on the apparent K_{IC} value at -196°C is shown in Fig. 8. Fractographic analysis showed that the martensite in the higher carbon steels (over 0.27%) had a tendency to fail by cleavage rather than by shear. The variation with carbon content of apparent K_{IC} values at -196°C reflects this change of fracture mode.

Gerberich et al. (1969) and Antolovich and Singh (1971) have derived analytical expressions which include the contribution of the phase transformation to the observed fracture toughness of TRIP steels. Both groups of investigators have concluded from theoretical and experimental evidence that the phase transformation is a major source of their fracture toughness. Antolovich and Singh (1971) experimentally determined this contribution to be between two-thirds and three-fourths of the measured crack extension force, G_{IC}. However, no attempt has yet been made (to the authors' knowledge) to estimate the change in stress state existing near the tip of a crack in a steel undergoing a stress- or strain-induced transformation. This is a very important factor. When austenite transforms to martensite, there is a volume

increase of about 3%. This corresponds to a linear increase of 1% in each of three perpendicular directions. This volumetric expansion effectively cancels a large part of the triaxial stress that exists near the root of a sharp crack or notch. The reduction in the triaxial component of stress has a marked effect on the behavior of thick specimens, where triaxiality is a major contributor to brittle behavior. As a consequence, TRIP steels exhibit an unusual variation in fracture toughness with specimen thickness. The fracture toughness of virtually all high strength alloys decreases sharply with increasing thickness. This does not appear to be the case with TRIP steels. As shown in Fig. 9, the critical stress intensity factors (K) at room temperature of both the low alloy quenched and tempered steel and the precipitation hardening stainless steel decrease with thickness more severely than those of the TRIP steel (Gerberich et al., 1971).

It has been shown both analytically and experimentally that the rate of production of strain induced martensite decreases with increasing crack velocity because of adiabiatic heating (Dokko, 1969, and Gerberich et al., 1971). The consequence is a decrease in the fracture toughness.

The powerful beneficial effect of the transformation of metastable austenite on the fracture toughness of steels apparently persists even when the metastable retained austenite is a minor constituent in a bcc iron matrix. This aspect of alloy design is discussed in the next section.

2. Quenched and Tempered Steels

Ultra-high strength steels are relatively brittle, and their mechanical properties are not sensitive to small changes in temperature and strain rate. Application of the fracture mechanics method of

analysis to alloy design is therefore natural (Knott, 1973). It should be recalled that the first rests on Irwin's pioneering concepts in fracture mechanics were made on this class of steels.

A voluminous literature now exists on both the macroscopic and microscopic aspects of fracture of ultra-high strength steels. No attempt is made in this report to review the literature in its entirety; rather, a few typical examples are used to illustrate progress made in the design of experimental steels with combinations of strength and toughness superior to those commercially available.

Several years ago, an extensive program was undertaken at the authors' laboratory on the fracture toughness of high strength steels. One principal objective in this study was to identify and characterize those elements of defect structure and microstructure that influenced the plane strain fracture toughness. It was surmised that some elements of structure would enhance, while others would degrade, the fracture toughness. In the planning phases of this program it was assumed that weak or brittle microconstituents would degrade fracture toughness while others might prove beneficial. For example, the lamellar or plate-like forms of ferrite and cementite which occur in pearlitic and upper bainitic microstructures were considered to be detrimental. Similarly, the presence of both non-metallic inclusions and undissolved brittle carbides was thought to be undesirable. Also, evidence suggested that twinned martensite plates, as opposed to untwinned plates or laths, were detrimental. On the beneficial side, there was speculation and some evidence that retained austenite might, under certain circumstances, improve the fracture toughness of high strength steels. Accordingly, a series of heat treatments was devised for both commercial and laboratory-type steels

with the objective of minimizing the deleterious compositional and structural features while maximizing the beneficial ones.

A critical phase in the heat treatment of any steel is the austenitizing step. During austenitization many compositional and structural changes occur and profoundly influence the final microstructure and its associated mechanical properties. For example, low austenitizing temperatures favor a small austenite grain size but may leave a larger fraction of brittle undissolved carbides. Conversely, high austenitizing temperatures lead to dissolution of a greater proportion of such carbides but cause a concomitant increase in austenite grain size. The complex and often unpredictable net effect of using a particular austenitizing temperature led, therefore, to a detailed study of its influence on the strength and toughness of a number of commercial and laboratory-type steels.

a. Austenitizing Temperature and Undissolved Alloy Carbides

As previously suggested, the presence of large undissolved particles of alloy carbides is likely to result in a deterioration of fracture toughness. The volume fraction and size of undissolved carbides left in the austenitic matrix prior to quenching, for a given composition, varies inversely with the austenitizing temperature. In an effort to evaluate relationships between austenitizing temperature, volume fraction of undissolved carbides, fracture toughness, and strength, several laboratory-type secondary hardening steels were studied. Their compositions are shown in Table II.

The effect of varying the austenitizing temperature on the room temperature yield strength, ultimate strength and the fracture toughness of as-quenched 0.30C-5Mo and 0.41C-5Mo steels is shown in Fig. 10 (T. Tom, 1973). In general, both strength and fracture toughness increased

with increase in the austenitizing temperature. The increase in fracture toughness with austenitizing temperature for the lower carbon steel was particularly striking. Metallographic examination of these high molybdenum steels indicated that extensive solution of alloy carbides occurred above a critical austenitizing temperature. The fracture toughness was observed to increase markedly in the same temperature range. Associated with the increased solution of carbides and the improved fracture toughness was, as expected, a pronounced increase in grain size. Similar experiments were performed with another set of lower alloy steels in which complete dissolution of carbides could be effected at austenitizing temperatures as low as 870°C. In this instance the fracture toughness of either steel was relatively independent of the austenitizing temperature (or grain size) as shown in Fig. 11.

Transmission electron microscopic studies using carbon replicas indicated that an austenitizing temperature of 870°C left undissolved carbides of approximately 0.05 microns in diameter for a 0.32C-2Mo steel, and of 1-3 microns for the 0.30C-5Mo steel, as shown in Figures 12 and 13, respectively. The deleterious effects of the larger carbides was suggested by the values of the ratio of plane strain fracture toughness to yield strength for the two steels in the as-quenched condition. These were 0.42 for the 0.32C-2Mo steel and 0.27 for the 0.30C-5Mo steel. Furthermore, the ratios were equal for the 0.32C-2Mo steel austenitized at 870°C and the 0.30C-5Mo steel austenitized at 1200°C. These results strongly indicated that the presence of hard, brittle undissolved particles above a certain critical size could lead to a significant degradation of the fracture toughness of alloy steels. The results also suggested that

the fracture toughness was insensitive to large variations in prior austenite grain size for those alloy steels whose matrix was free of undissolved carbides of sizes above a critical value. Additional information on these steels is found in the investigations of Goolsby (1971) and T. Tom (1973).

b. Austenitizing Temperature and Hardenability

The foregoing discussion showed that using relatively high austenitizing temperature dissolved a greater proportion of alloy carbides and that this was usually associated with a large increase in prior austenitic grain size. Both the above phenomena tend to increase hardenability, i.e., either a thicker section can be through-hardened for a given quenching rate, or, alternatively, a slower quenching rate may be used for a given section size without encountering the usually undesirable microstructural effects of metastable austenite decomposition. Austenitizing temperatures higher than those conventionally employed may therefore be used: (1) to enhance the hardenability of low alloy steels, and (2) to promote the presence of desirable phases for enhanced fracture toughness, such as retained austenite. An example of each of these possibilities is discussed in the following section (see also Katz, 1961 and 1965).

The room temperature plane strain fracture toughness of a relatively low hardenability steel, AISI 4130, is shown in Fig. 14 as a function of tempering temperature for several austenitizing treatments. The tempering response of this steel and others as a function of austenitizing temperature is discussed in a subsequent section. The plane strain fracture toughness of the as-quenched steel varies markedly with austenitizing temperature and severity of quench. An austenitizing temperature of 1200°C

followed by an ice-brine quench and refrigeration in liquid nitrogen (IBQLN) resulted in nearly a two-fold increase in room temperature fracture toughness compared to that obtained by the conventionally recommended heat treatment of austenitizing at 870°C and oil quenching. A somewhat slower quench from 1200°C, i.e., oil quench vs. ice-brine, also improved the toughness relative to the commercial heat treatment but not so much as the more severe quench. Associated with the increases in fracture toughness were corresponding microstructural changes, as shown in Fig. 15 (a) and (b). The microstructure of a fracture toughness specimen oil quenched from 870°C consisted of a mixture of blocky ferrite and martensite, as shown in Fig. 15 (a). Extensive transmission electron microscopy using thin foils revealed that some of the martensite was autotempered. The microstructural appearance of a specimen ice-brine quenched from 1200°C was quite different, viz., there was virtually no evidence of ferrite, as shown in Fig. 15 (b). A similar correspondence between heat treatment, fracture toughness and microstructure existed for steel AISI 4330. Plots of plain strain fracture toughness vs. tempering temperature for two austenitizing treatments are shown in Fig. 16. Additional information on these steels is found in the investigations of Wood et al. (1973).

Unconventional heat treatments of the kind described above for steels of high hardenability resulted in similar improvements in fracture toughness even though there appeared to be no corresponding microstructural changes except the expected grain size differences, as determined by optical metallographic observations. The room temperature plane strain fracture toughness of AISI 4340 steel is plotted in Fig. 17 as a function of tempering temperature for two austenitizing treatments. The

preferred heat treatment involves a step-quench from 1200°C to 870°C followed by an oil quench. Quench cracking occurred in the steel when it was quenched from the higher temperature or if a quench more drastic than oil was used. As can be seen from Fig. 17 the plane strain fracture toughness of the as-quenched steel was nearly doubled by the step-quench heat treatment. Examination of the microstructures by transmission electron microscopy of specimens given both types of heat treatment revealed differences in the amount of retained austenite and in the nature of the substructure. As shown in the bright and dark field transmission micrographs of the specimen conventionally heat treated, the amount of retained austenite (revealed by use of an austenite reflection) was small, as shown in Fig. 18 (a) and (b). In contrast, the same metallographic technique revealed extensive networks of retained austenite --- in some areas of the specimen almost every martensite plate and lath was surrounded by austenite films that were 100-200 Å thick, as shown in Fig. 19 (a) and (b).

Transmission electron microscopy revealed another distinct microstructural difference between specimens given the two heat treatments. The packets of lath martensite were very similar for both austenitizing treatments. However, twinned martensite plates were observed in the conventional treatment only; the use of the step-austenitizing treatment apparently resulted in the virtual elimination of twinned martensite plates, as shown in a comparison of Figs. 20 (a) and (b). A detailed discussion of the role of these various changes in the microstructure and their possible effects on fracture toughness is found in a paper by

Lai et al. (1974). Briefly, it appears that both the presence of retained austenite, especially in the observed morphology, and the absence of twinned martensite plates favor the fracture toughness of specimens given the step-austenitizing heat treatment. Webster (1968 and 1971) and Antolovich et al. (1974) have suggested that retained austenite may enhance the fracture toughness of high strength steels by either blunting an advancing crack or by undergoing a strain- or stress-induced transformation at the advancing crack tip. The consequences of the latter have been considered by Gerberich et al. (1971) and Antolovich and Singh (1971), as well as by Zackay et al. (1973). Das and Thomas (1969), Thomas (1971), and Thomas and Das (1971) have comprehensively treated the problem of twinned martensite plates as they influence the fracture toughness of ultra-high strength steels. With the existing information, it is not possible to establish the individual or combined role of these microstructural features on the fracture toughness of complex high strength steels. The need for definitive solutions of these and other problems in the design of new and superior steels is discussed in a later section.

c. Austenitizing Temperature and Tempering Response

In the foregoing discussion, attention was centered on the effects that variations in the austenitizing temperature can have on the plane strain fracture toughness of as-quenched steels. It was shown that these effects, whether beneficial or detrimental, could usually be traced to the appearance or disappearance of some element of microstructure or substructure. The same can be said of the tempering response, although the causal relationships are less clear and are dependent in some cases upon subtle combined chemical and mechanical effects which appear to take place on a sub-microscopic scale.

The influence on tempering with variations in austenitizing temperature and severity of quench was shown earlier for several commercial steels, viz., Fig. 14 for AISI 4130 steel, Fig. 16 for AISI 4330 steel, and Fig. 17 for AISI 4340 steel. The chemical composition of these steels and one other --- the 300-M steel, are shown in Table III. The last mentioned steel is a modified version of AISI 4340 steel containing 0.08% vanadium and 1.59% silicon. A comparison of Figures 14, 16, and 17 reveal that the use of higher austenitizing temperatures resulted in tempered martensite embrittlement for the AISI 4130 and 4340 steels in tempering range of 200-350°C. This type of embrittlement was not observed for the AISI 4330 and 300-M steels treated at the high austenitizing temperature or for any of the steels conventionally heat treated. The fracture of the embrittled specimens was intergranular along prior austenite grain boundaries, while that of unembrittled specimens (either in the as-quenched condition or tempered at 200°C) occurred by dimpled rupture. No significant microstructural differences could be detected by transmission electron microscopy between the embrittled and the unembrittled specimens. The only compositional difference between the embrittled and unembrittled steels was the presence of vanadium in the latter. Several possible causes of the observed change in fracture mode have been discussed in detail by Lai _et al_. (1974). One of the possible mechanisms for this type of embrittlement is the presence of certain impurity elements as suggested by Capus and Mayer (1960), Low (1969), Kula and Anctil (1969), and Ohtani _et al_. (1974), among others. Kula and Anctil suggest that when cementite grows at prior austenite grain boundaries during tempering, such impurity elements as phosphorus, which are probably more soluble in

ferrite than in cementite, will diffuse out of the cementite into the surrounding ferrite. A film of segregated impurities might build up at the interface between ferrite and cementite. The presence of the film may then result in a lowering of the interfacial energy and provide a low-energy path for intergranular fracture. Ohtani et al. (1974) have suggested a similar mechanism for temper embrittlement. These workers contend that the classic equilibrium segregation theory of temper embrittlement may have to be discarded. In accordance with their model, stabilization of carbides by elements such as molybdenum or vanadium is a possible way of suppressing embrittlement. The experimental results presented in this section on the tempering response of vanadium-containing and vanadium-free commercial steels subjected to high austenitizing temperatures are therefore not inconsistent with the Kula and Anctil model for tempered martensite embrittlement.

Finally, no review of impurity effects on the toughness of high strength steels should exclude mention of the deleterious influences of sulfur and phosphorus. A recent representative study in this field was that of Birkle et al. (1966), who examined the relationship between the density and distribution of sulfide inclusions and plane strain fracture toughness. The effect of the sulfur level on the fracture toughness of 0.45C-Ni-Cr-Mo steels is shown in Fig. 21, from Birkle et al., (1966). The authors conclude from fractographic studies that the crack growth process consists of the growth and coalescence of voids nucleated by sulfide inclusions and carbide particles. The average spacings between the sulfide inclusions decreased with increasing sulfur content and correlated well with the "process zone" sizes computed using a model

by Krafft (1964) in which the onset of plane strain fracture instability is related to the tensile plastic flow instability in a small zone of material ahead of the crack tip.

In a study of the role of impurity elements (P, S, Cu, As, Sn) on the critical flaw size for catastrophic fracture, Cottrell (1970) stressed the importance of the synergistic influence of impurities. For example, the combined effect of As and S in degrading fracture toughness was far greater than the sum of their individual effects. As might be expected, the most serious deterioration of toughness was observed at a tempering temperature when both temper embrittlement (dependent on tempering temperature) and sulfide embrittlement (largeley independent of tempering temperature) occurred.

It may be concluded from these few representative studies that impurity levels and types have major influences on the plane strain fracture toughness of ultra-high strength steels. As Cottrell points out in his paper, the effect of purification on the critical defect size, in a conventional low alloy steel with a yield strength of 240,000 psi, may be far greater than that achieved by the alternative route of the substitution of the low alloy steel with a maraging steel. Darmara (1967) has reviewed some then current and proposed methods of purifying steel. It is clear from his remarks and from the continuing high level of activity in this area that the steel-making processes of the future will produce steels with combinations of mechanical properties that are achieved now only in the controlled purity alloys of the research laboratory.

C. An Important Unsolved Problem

The alloying elements of steel and the solid state reactions which they undergo determine the structure and, therefore, the properties of steel. The complex nature of these reactions is not yet fully understood and an understanding of the nature of these reactions important in the economic design of superior steels. For example, even if the influences of all the common alloying elements were individually known on the thermodynamics and kinetics of the principal isothermal reactions of plain carbon steels, the information would be insufficient for the effective design of complex steels because commercial steels contain many interacting elements whose total effect is often different from that predicted on the basis of the individual elements alone. A real need exists therefore for a technique for rapidly predicting the single and the combined effects of all the common alloying elements on the solid state metallurgical reactions that are important in the heat treatment of steel. Knowing the initiation (incubation) and finish times of these reactions and their associated kinetics is particularly important. Progress made in the authors' laboratory in developing such a technique is described below.

The rapid method of studying the isothermal reactions in steels consists in quenching the steel sample from the austenitizing temperature to a subcritical temperature in an isothermal bath and holding it within the magnetic field of an inductor coil. The increase in permeability accompanying austenite decomposition increases the inductance of the coil, and this changes the resonant frequency of the circuit. An automatic continuous recording of the corresponding period provides a convenient

and accurate method for following the austenite decomposition. Quantitative information on austenite decomposition kinetics can be obtained within two seconds after the start of quenching (Babu et al., 1973; and Ericsson et al., 1974). An example illustrating some of the preliminary results obtained by this method is described below.

In the recently reported T-T-T diagrams for AISI 4340 steel, the bainite range is shown as a smooth C-shaped curve, Fig. 22 (a). Investigations by the new method showed significant differences in the shape and character of the lower bainite region. As shown in Fig. 22 (b), the incubation period for the formation of lower bainite decreased at temperatures just above M_s and gave an S-shaped curve for the bainite reaction. This acceleration of austenite decomposition at temperatures just above M_s has been observed previously (Howard and Cohen, 1948; Schaaber, 1955; and Radcliffe and Rollason, 1959).

That part of the lower bainite curve which extended below the M_s had a C-shape, as shown in Fig. 22 (b). Immediately below the M_s, the bainite reaction began almost instantly after the end of the martensite reaction. This rapid onset at temperatures just below the M_s is well established in the literature and is associated with the increased nucleation of the bainite reaction by the strain effects associated with the austenite to martensite transformation. The decreased rate of bainite formation at temperatures well below the M_s was apparently due to the lower diffusion rates of carbon.

Reactions of the type described above and their associated microstructures have meaning for both the user of existing commerical steels and the designer of new ones. To the user of commercial steels,

the precise location and shape of the lower and upper bainite reaction curves is significant from a hardenability viewpoint. Avoiding certain cooling rates can prevent the formation of upper bainite, an undesirable microstructure for mechanical properties. This is especially important in complex parts with varying section sizes. To the designer of new steels, knowledge of the details of the lower bainite and martensite reactions presents an opportunity to evaluate the mechanical properties of steels with the unusual mixed microstructures of lower bainite, autotempered and tempered martensite, and retained austenite. It is hoped that this new experimental technique for the rapid determination of T-T-T diagrams, coupled with basic studies of austenite decomposition on simplerhigh purity steels such as those, for example, of Aaronson and Domian (1966) and Hehemann et al. (1972), will eventually provide the basis for designing complex steels that are both economical and superior in properties to those currently available.

ACKNOWLEDGMENTS:

The authors are grateful to Dr. Michael Yokota, Dr. George Lai, Dr. William Wood, Dr. Thomas Tom and Mr. Naga Prakash Babu for use of unpublished data, and to Dr. M. Dilip Bhandarkar for his many discussions and critical technical review.

This work was performed under the auspices of the United States Atomic Energy Commission through the Inorganic Materials Research Division of the Lawrence Berkeley Laboratory. Additional support was received from the Army Materials and Mechanics Research Center, Watertown, Massachusetts.

References

Aaronson, H. I., and Domian, H.A. (1966). Trans. Met. Soc. AIME, 236, 781-796.

Angel, T. (1954). J. Iron Steel Inst., 177, 165-174.

Antolovich, S. D. (1968) Trans. Met Soc. AIME, 242, 2371-2373.

Antolovich, S. D. and Singh, B. (1971). Met. Trans., 2, 2135-2141.

Antolovich S. D.,Saxena, A., and Chanani, G. R. (1974). Met. Trans., 5, 623-632.

Averback, B. L. (1968). In "Fracture" (H. Liebowitz, ed.), Vol. I, pp. 441-472, Academic Press, New York.

Babu, B. N. P., Ott, D.,Parker, E. R., and Zackay, V. F. (1973). LBL-2502, In preparation, Lawrence Berkeley Laboratory, Berkeley, California.

Bhandarkar, D., Zackay, V. F., and Parker, E. R. (1972). Met. Trans., 3, 2619-2631.

Birkle, A. J., Wei, R. P., and Pellissier, G. E. (1966). Trans. ASM, 59, 981-990.

Bressanelli, J. P., and Moskowitz, A. (1966). Trans. ASM, 59, 223-239.

Capus, J. M., and Mayer, G. (1960). Metallurgia, 62, 133-138.

References contd.

Cottrell, C. L. M. (1970). In "Fracture Toughness of High Strength Materials: Theory and Practice," ISI Publication 120, p. 112-115, The Iron and Steel Institute, London.

Darmara, F. N. (1967). J. Metals, 19 (12), 42-48.

Das, S. K., and Thomas G. (1969). Trans. ASM, 62, 659-676.

Dokko, C. (1969). M. S. Thesis, UCRL-19068, University of California, Berkeley, California.

Ericsson, C. E., Parker, E. R., and Zackay, V. F. (1974). In preparation, Lawrence Berkeley Laboratory, Berkeley, California.

Fahr, D. (1969). Ph.D. Thesis, UCRL-19060, University of California, Berkeley, California.

Fahr, D. (1971). Met. Trans., 2, 1883-1892.

Gerberich, W. W., and Birat, J. P. (1971). Int. J. Fract. Mech., 7, 108-110.

Gerberich, W. W., Hemmings, P. L., Merz, M. D., and Zackay, V. F. (1968). Trans. ASM, 61, 843-847.

Gerberich, W. W., Hemmings, P. L., Zackay, V. F., and Parker, E. R. (1969). In "Fracture 1969" (P. L. Pratt, ed.), pp. 288-305, Chapman and Hall, Ltd., London.

References contd.

Gerberich, W. W., Thomas G., Parker, E. R., and Zackay, V. F. (1970). In Proc. 2nd Int. Conf. Strength of Metals and Alloys, Asilomar, California, 1970, 3, 894-899.

Gerberich, W. W.,Hemmings, P. L., and Zackay, V. F. (1971). Met. Trans., 2, 2243-2253.

Goolsby, R. D. (1971). Ph.D. Thesis, LBL-405, University of California, Berkeley, California.

Hehemann, R. F.,Kinsman, K. R., and Aaronson, H. I. (1972). Met. Trans., 3, 1077-1094.

Horwood, W. A. (1972). M.S. Thesis, LBL-1121, University of California, Berkeley, California.

Howard, R. T., Jr., and Cohen, M. (1948). Trans. AIME, 176, 384-397.

Jin, S., Horwood, W. A., Morris, J. W., Jr., and Zackay, V. F. (1973a). Advan. Cryog. Eng. In press.

Jin, S. , Morris, J. W., Jr., and Zackay, V. F. (1973 b). Advan. Cryog. Eng. In press.

Jin, S., Morris, J. W., Jr., and Zackay, V. F. (1973 c). Presented at Materials Engineering Congress, Chicago, Illinois, October 1973.

Katz, R. N. (1961), Tech. Note WAL TN 320.1/8, Watertown Arsenal, Watertown, Mass.

Katz, R. N. (1965). Tech. Note AMRA TN 65-09, Materials Engineering Division, U. S. Army Materials Research Agency, Watertown, Mass.

Knott, J. F. (1973). "Fundamentals of Fracture Mechanics," Butterworths, London.

Krafft, J. M. (1964). Appl. Mater. Res., 3, 88-101.

Kula, E. B. and Anctil, A. A. (1969). J. Mater. 4(4), 817-841.

Kulin, S. A. Cohen, M., and Averback, B. L. (1952). Trans. AIME, 194, 661-668.

Lai, G. Y., Wood, W. E., Parker, E. R., and Zackay, V. F. (1974). In preparation.

Liebowitz, H. (1968), ed. "Fracture," Vol. I-VII, Academic Press, New York.

Loss, F. J. and Pellini, W. S. (1969). In "Practical Fracture Mechanics for Structural Steel," Paper J, UKAEA, Chapman and Hall, London.

Low, J. R., Jr. (1969). Trans. Met. Soc. AIME, 245, 2481-2494.

Ohtani, H., Geng, H. C., and McMahon, C. J., Jr. (1974). Met. Trans., 5, 516-518.

Osborn, C. J., Gifkins, R. C., Hoggart, J. S., and Mansell, D. S. (1969), eds. "Fracture," Proc. 2nd Tewksbury Symp., Fac. Eng. Univ. Melbourne, Melbourne, Australia.

Pellini, W. S. (1968). NRL Report 6713, April 3, Naval Research Laboratory, Washington, D.C. Also, Welding Research Council Bulletin, 130, May 1968.

Puzak, P. P., and Lange, E. A. (1969). NRL Rep. 6951, Sept. 18, Naval Research Laboratory, Washington, D.C.

Radcliffe, S. V., and Rollason, E. C. (1959). J. Iron Steel Inst., 191, 56-65.

Sasaki, G. (1973). D. Eng. Thesis, LBL-1493, University of California, Berkeley, California.

Sasaki, G. Yokota, M. J., and Zackay, V. F. (1974). In preparation, Lawrence Berkeley Laboratory, Berkeley, California.

Schaaber, O. (1955). Trans. AIME, 203, 559-560.

Scheil, E. (1932). Z. Anorg. Allg. Chem., 207, 21-40.

Tamura, I., Maki, T., Hato, H., Tomoto, Y., and Akada, M. (1970). In Proc. 2nd Int. Conf. Strength of Metals and Alloys, Asimolar, California 1970, 3, 900-904.

Tetelman, A. S., and McEvily, A. J., Jr. (1967). "Fracture of Structural Materials," John Wiley and Sons, Inc., New York.

Thomas, G. (1971). Met. Trans., 2, 2373-2385.

Thomas G., and Das, S. K. (1971). J. Iron Steel Inst., 209,801-804.

Tom, T. (1973), D. Eng Thesis, LBL-1856, University of California, Berkeley, California.

Webster, D. (1968). Trans. ASM, 61, 816-828.

Webster, D. (1971). Met. Trans., 2, 2097-2104.

Wood, W. E., Parker, E. R., and Zackay, V. F. (1973). LBL-1474, Lawrence Berkeley Laboratory, Berkeley, California.

Yakota, M. J., Sasaki, G., Horwood, W. A., Zackay, V.F., and Parker, E. R., (1974 a). LBL-2278, in preparation, Lawrence Berkeley Laboratory, Berkeley, California.

Zackay, V. F., Parker, E. R., Fahr, D., and Busch, R. (1967). Trans. ASM, 60, 252-259.

Zackay, V. F. (1973). In "Microstructure and Design of Alloys," pp. 591-595, Institute of Metals, London.

TABLE I

CHEMICAL COMPOSITIONS OF TRIP STEELS

Designations	Compositions, Wt.%			
	C	Ni	Cr	Mn
CN8Cr	0.325	8.0	9.0	2.0
CN12Cr	0.290	12.0	9.0	2.0
CN16Cr	0.292	16.0	9.0	2.0
CN21Cr	0.287	21.4	9.0	2.0

TABLE II

CHEMICAL COMPOSITIONS OF C-Mo STEELS

Designations	Compositions, Wt.%					
	C	Mo	Ni	Mn	S	P
0.34C-1Mo	0.34	0.95	---	0.63	0.005	0.008
0.30C-2Mo	0.32	1.96	---	0.65	0.005	0.007
0.30C-5Mo	0.30	5.03	---	0.60	0.005	0.008
0.41C-5Mo	0.41	4.93	---	0.51	0.005	0.007
0.35C-1Mo-3Ni	0.35	0.95	3.1	0.61	0.005	0.007
0.35C-2Mo-3Ni	0.35	1.90	3.1	0.67	0.005	0.007

Sn, Sb < 0.002%, As < 0.005% and

Si < 0.02% in all steels.

TABLE III

CHEMICAL COMPOSITION OF LOW ALLOY STEELS

STEEL	Compositions, Wt.%									
	C	Mn	Cr	Ni	Mo	S	Si	Cu	P	V
AISI 4130-A	0.31	0.57	0.85	0.15	0.18	0.009	0.28	0.21	0.008	<0.005
AISI 4130-B	0.33	0.63	0.90	0.15	0.18	0.009	0.27	0.19	0.008	<0.005
AISI 4330	0.28	1.02	0.85	1.80	0.40	0.005	0.28	0.10	0.009	0.07
AISI 4340	0.40	0.85	0.72	1.73	0.26	0.010	0.22	0.14	0.004	<0.005
300-M	0.41	0.79	0.75	1.85	0.43	0.002	1.59	0.04	0.008	0.08

Figure Captions

Fig. 1. Plots of Charpy V-notch impact energy at -196°C vs. reheating temperature for Fe-12Ni-0.5Ti alloy. The heat treatments are indicated.

Fig. 2. Relationship between prior austenite grain size and Charpy impact energy at -196°C for the Fe-12Ni-0.5Ti alloy.

Fig. 3. The relation between engineering strain and the volume fraction of martensite that is produced in steel CN8Cr, deformed 70% at 450°C, when tested at a temperature of -78°C.

Fig. 4. The engineering stress-strain curves of steel CN8Cr, deformed 70% at 450°C (PDA is an abbreviation for prior deformation of austenite), tested at 22°C and -78°C. The values of the stability coefficient, m, are shown.

Fig. 5. The engineering stress-strain curves for steels containing 8, 12, and 16% nickel, deformed 70% at 450°C and tested at -78°C. The values of the stability coefficient, m, are shown.

Fig. 6. The correlation between the stability coefficient, m, and (a) the elongation to fracture, and (b) Lüders strain. Data were obtained from a large group of metastable austenitic steels of widely varying composition, processing histories, and testing temperatures.

Fig. 7. Influence of austenite stability (m value) on the plane stress fracture toughness of high strength metastable austenites.

Fig. 8. Effect of carbon and nitrogen contents on cleavage of martensite and hence on apparent K_{IC}, at -196°C.

Fig. 9. Influence of thickness on the critical stress intensity factors at room temperature for a TRIP steel and two commercial steels.

Fig. 10. Plots showing the influence of austenitizing temperature on room temperature fracture toughness (K_{IC} or K_Q), yield strength (Y.S.), and ultimate strength (U.S.) of 0.30C-5Mo and 0.41C-5Mo steels.

Fig. 11. Plots of room temperature plane strain fracture toughness vs. prior austenite grain size (indicated by ASTM grain size number) for as-quenched 0.34C-1Mo and 0.35C-1Mo-3Ni steels.

Fig. 12. Transmission electron micrograph of a carbon replica showing fine undissolved carbides in as-quenched 0.32C-2Mo steel, austenitized at 870°C.

Fig. 13. Transmission electron micrograph of a carbon replica showing 1-3 micron size undissolved carbides in as-quenched 0.30C-5Mo steel, austenitized at 870°C.

Fig. 14. Plots of room temperature plane strain fracture toughness vs. tempering temperature for AISI 4130 steel. Austenitizing temperatures and quenching media are indicated.

Fig. 15. Microstructure of AISI 4130 steel: (a) austenitized at 870°C and oil quenched (arrows indicate ferrite and upper bainite), and (b) austenitized at 1200°C and ice-brine quenched.

Fig. 16. Plots of room temperature plane strain fracture toughness vs. tempering temperature for AISI 4330 steel. Austenitizing temperatures and quenching media are indicated.

Fig. 17. Plots of room temperature plane strain fracture toughness vs. tempering temperature for AISI 4340 steel. Austenitizing temperatures and quenching media are indicated.

Fig. 18. Transmission electron micrographs of as-quenched AISI 4340 steel: (a) bright field and (b) dark field of austenite reflection for the 870°C austenitized specimen.

Fig. 19. Transmission electron micrographs of as-quenched AISI 4340 steel: (a) bright field and (b) dark field of austenite reflection for the 1200°C → 870°C austenitized specimen.

Fig. 20. Transmission electron micrographs of martensite plates in AISI 4340 steel: (a) austenitized at 870°C, showing extensive fine transformation twins in a martensite plate marked P, (b) austenitized at 1200°C, showing absence of transformation twins and presence of ε carbides in a cross-hatched morphology in martensite plates marked P. A prior austenite grain boundary is marked GB.

Fig. 21. Influence of sulfur level on plain strain fracture toughness and strength of quenched and tempered 0.45C-Ni-Cr-Mo steels (from Birkle *et al.*, 1966).

Fig. 22. T-T-T diagrams of AISI 4340 steel: (a) as reported in the literature, and (b) as determined by the new magnetic permeability technique.

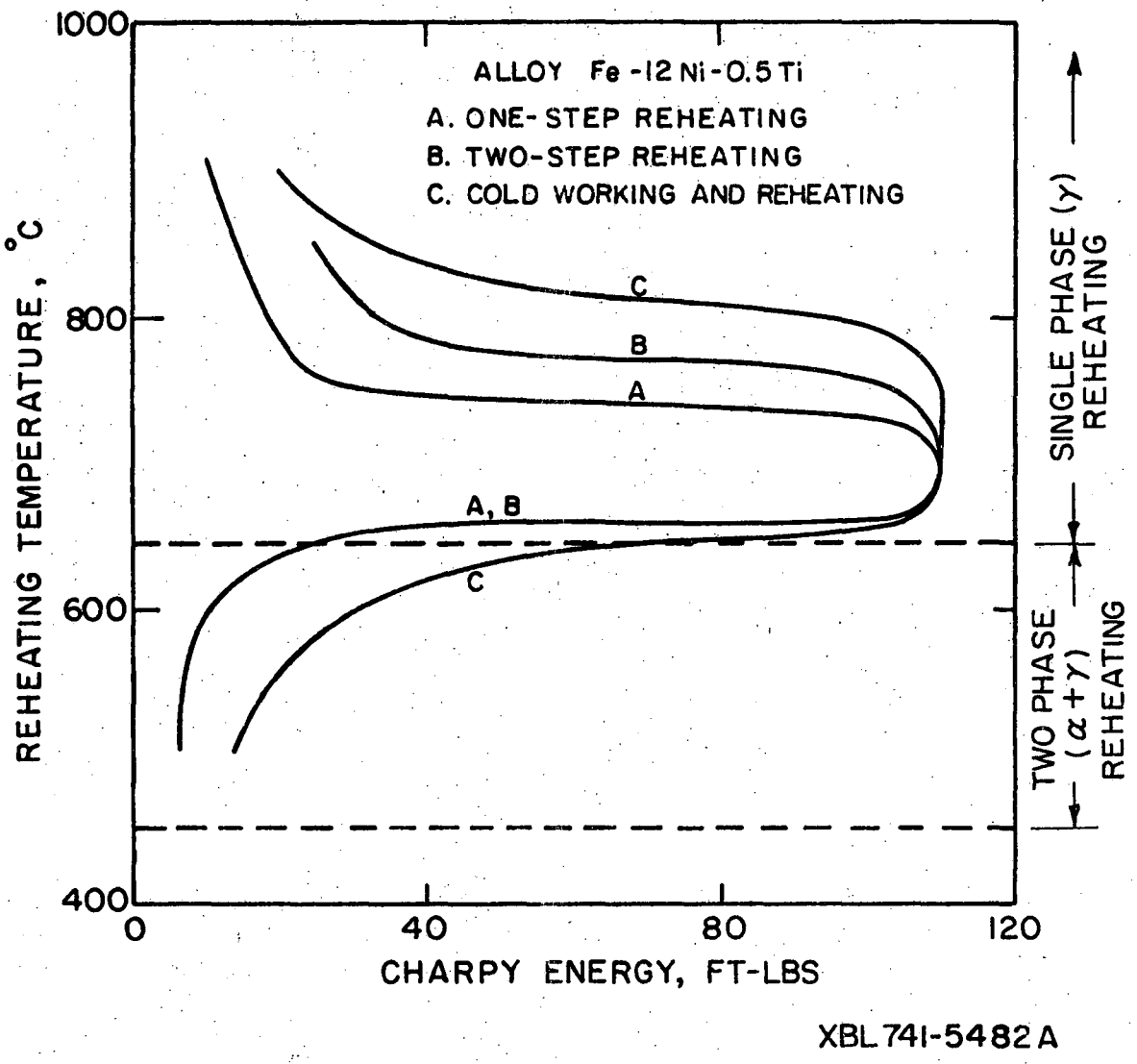
ALLOY Fe-12Ni-0.5Ti
A. ONE-STEP REHEATING
B. TWO-STEP REHEATING
C. COLD WORKING AND REHEATING
C
B
A
A, B
C
REHEATING TEMPERATURE, °C
1000
800
600
400
0
40
80
120
CHARPY ENERGY, FT-LBS
SINGLE PHASE (γ) REHEATING
TWO PHASE (α+γ) REHEATING
XBL 741-5482A

Fig. 1

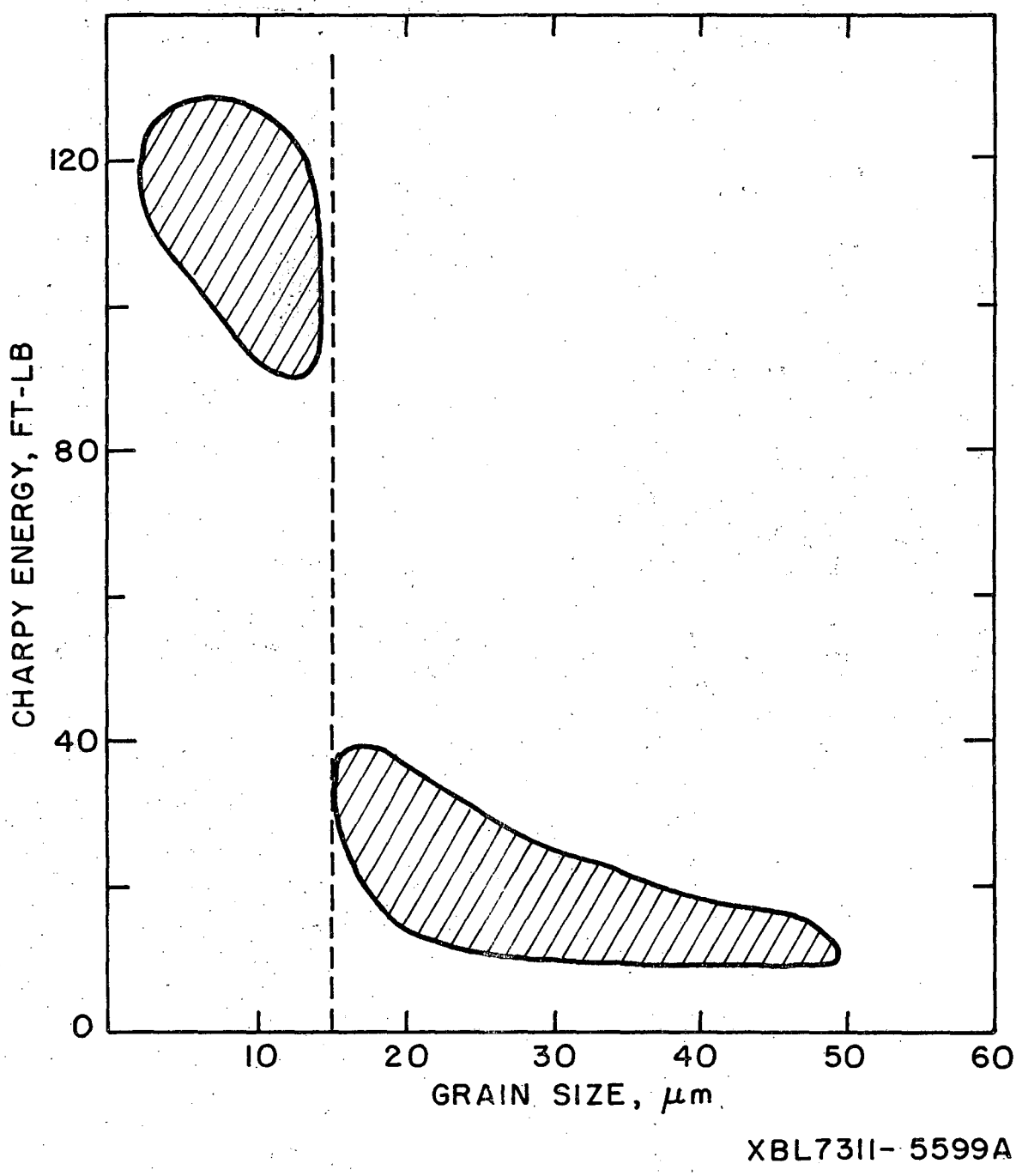
120
80
40
0
CHARPY ENERGY, FT-LB
10
20
30
40
50
60
GRAIN SIZE, μm
XBL7311-5599A

Fig. 2

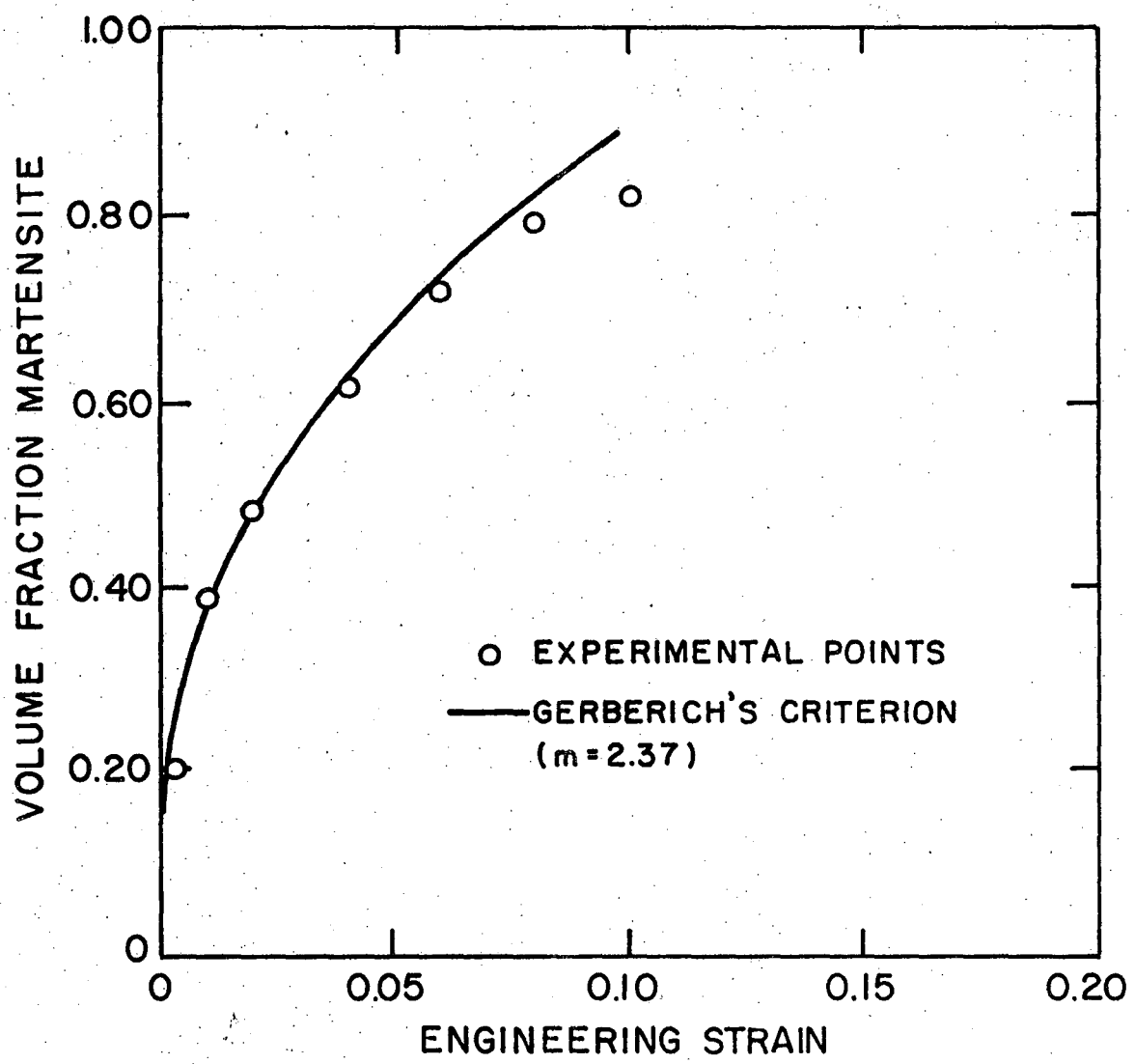

XBL 7110-7501A

Fig. 3

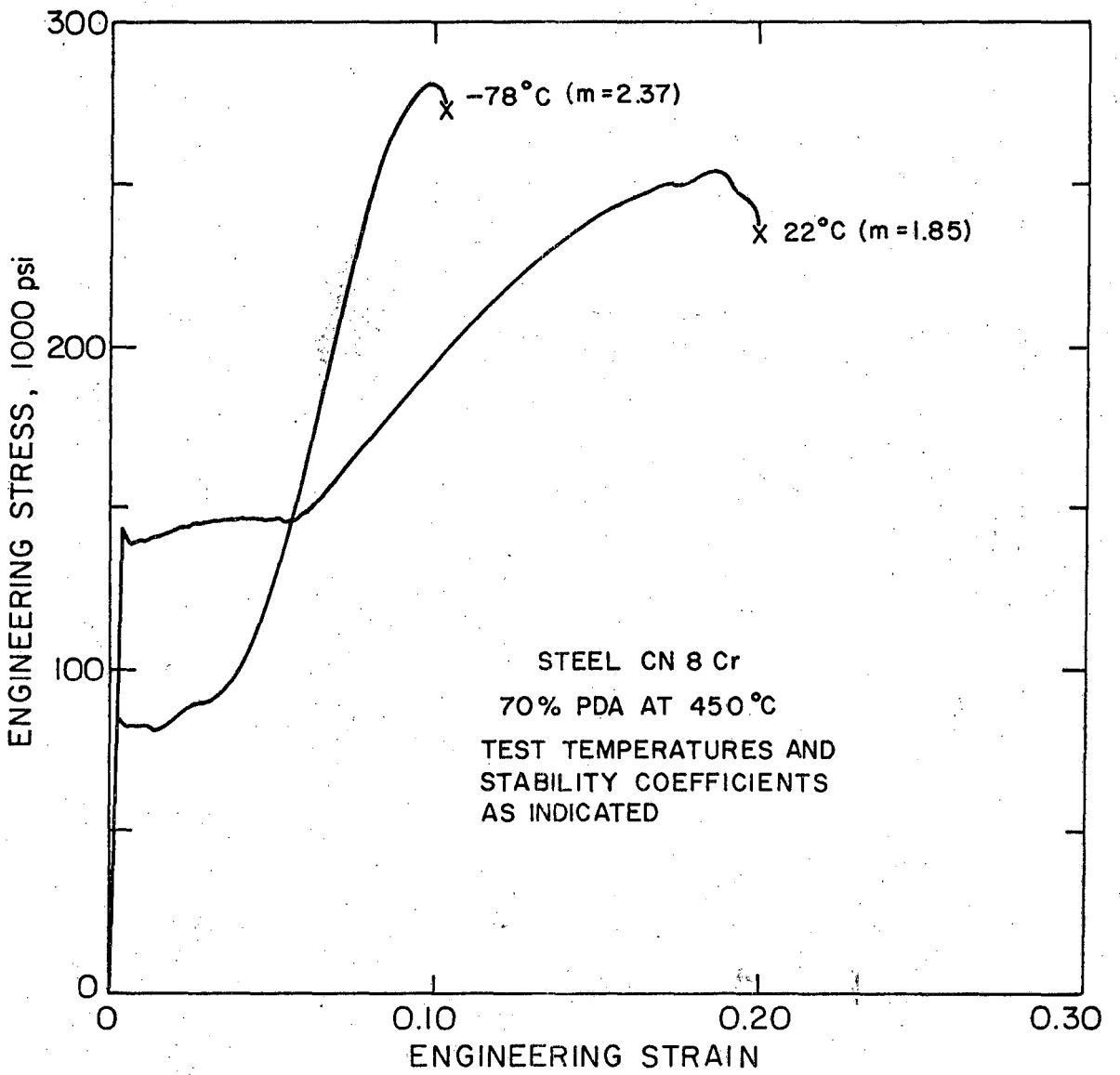

XBL7110-7504A

Fig. 4

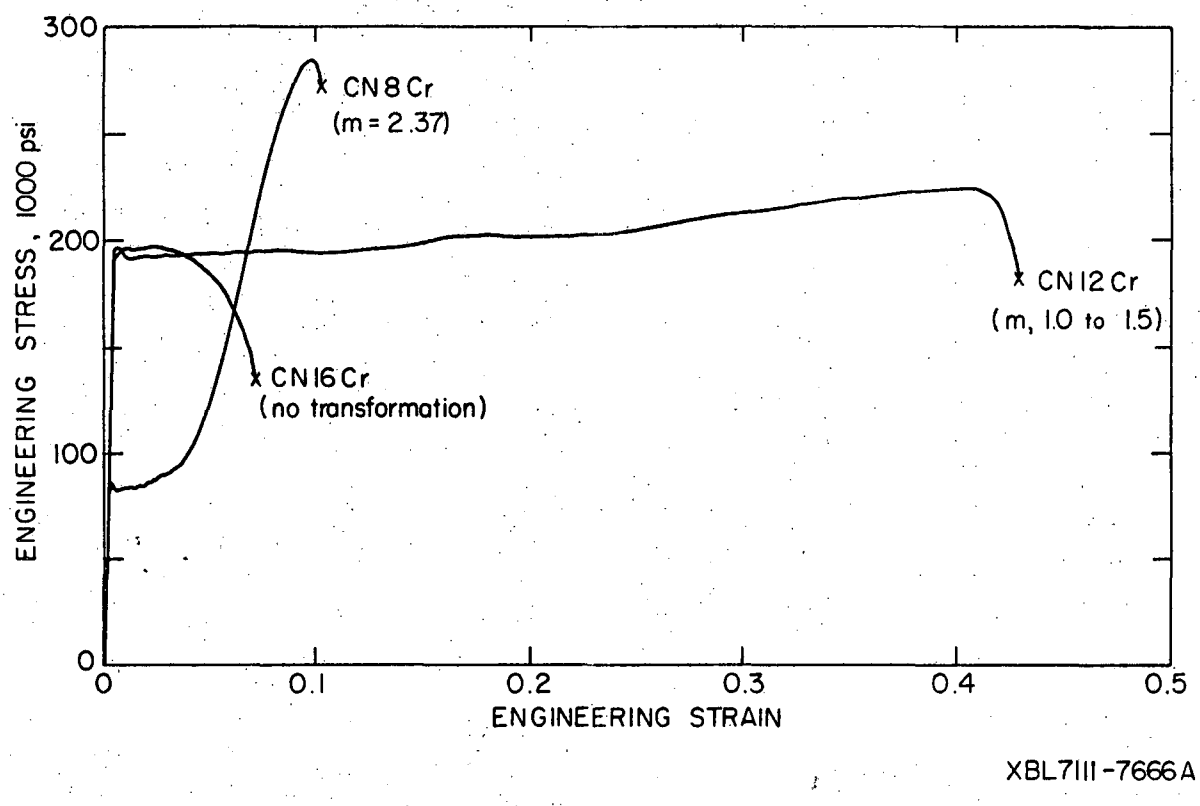
300
200
100
0
ENGINEERING STRESS, 1000 psi
0
0.1
0.2
0.3
0.4
0.5
ENGINEERING STRAIN
CN 8 Cr
(m = 2.37)
CN 12 Cr
(m, 1.0 to 1.5)
CN 16 Cr
(no transformation)
XBL7111-7666A

Fig. 5

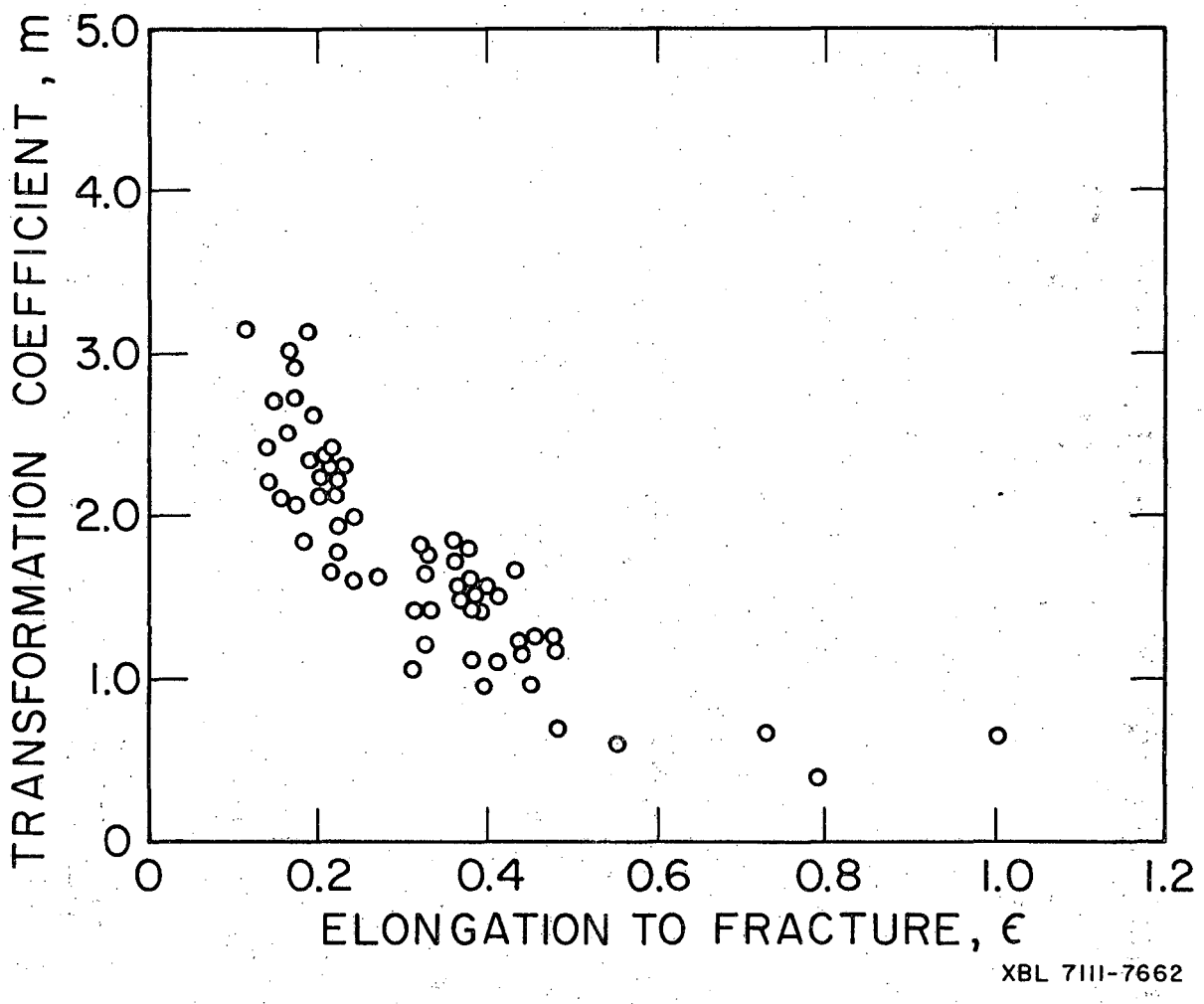
TRANSFORMATION COEFFICIENT, m
5.0
4.0
3.0
2.0
1.0
0
0
0.2
0.4
0.6
0.8
1.0
1.2
ELONGATION TO FRACTURE, ε
XBL 7111-7662

Fig. 6(a)

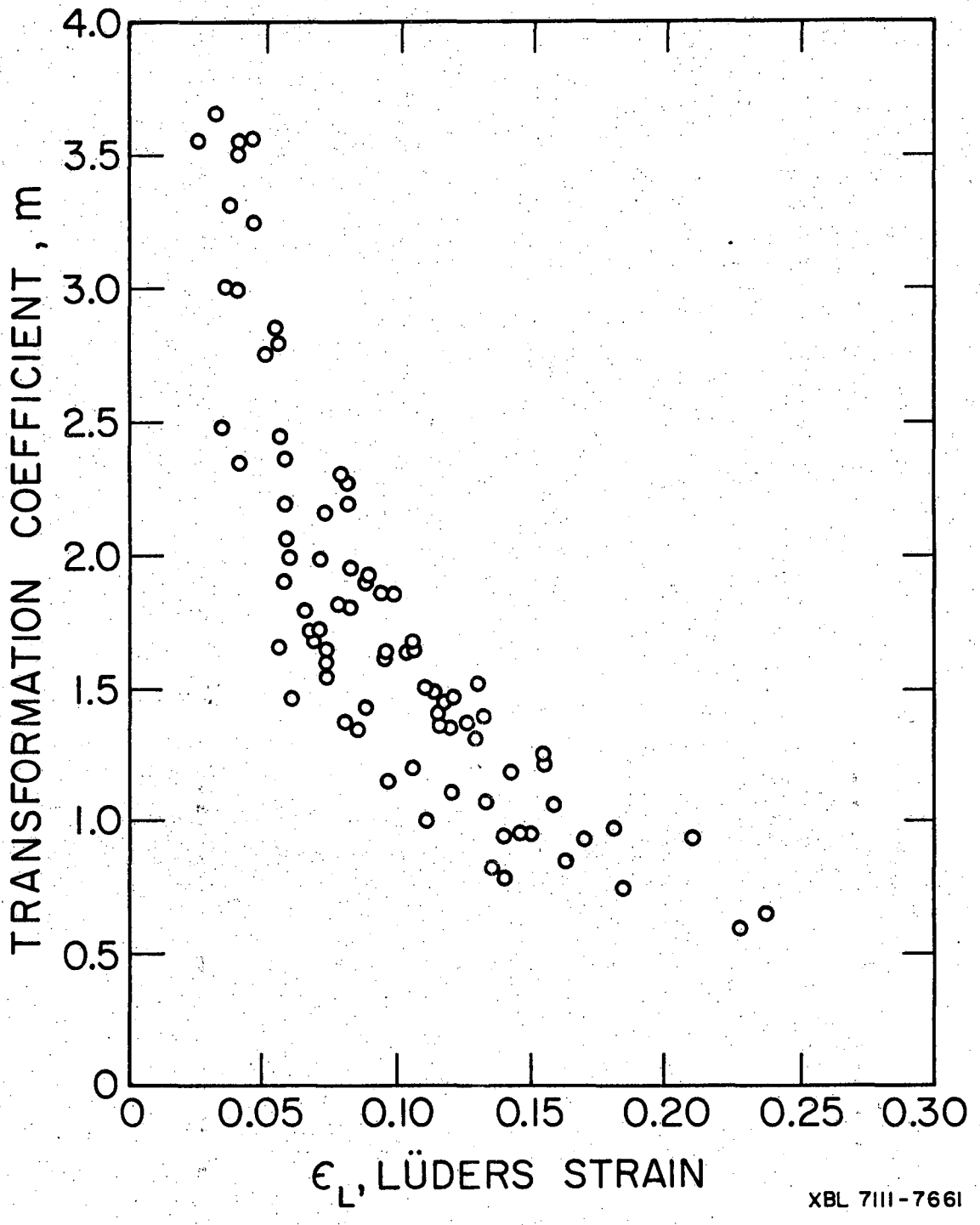
4.0
3.5
3.0
2.5
2.0
1.5
1.0
0.5
0
TRANSFORMATION COEFFICIENT, m
0
0.05
0.10
0.15
0.20
0.25
0.30
ϵ_L, LÜDERS STRAIN
XBL 7111-7661

Fig. 6(b)

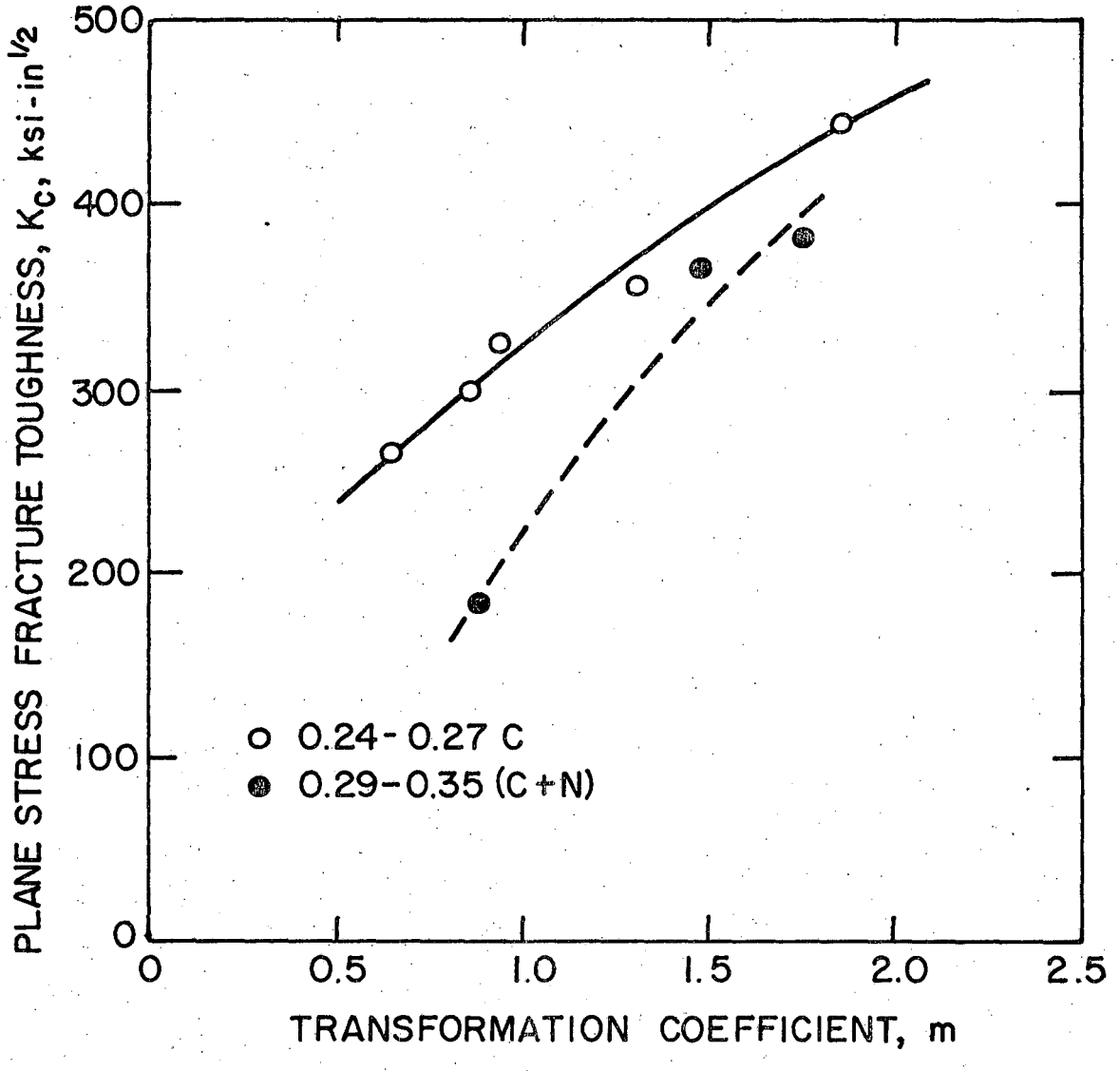

XBL 7011-6952A

Fig. 7

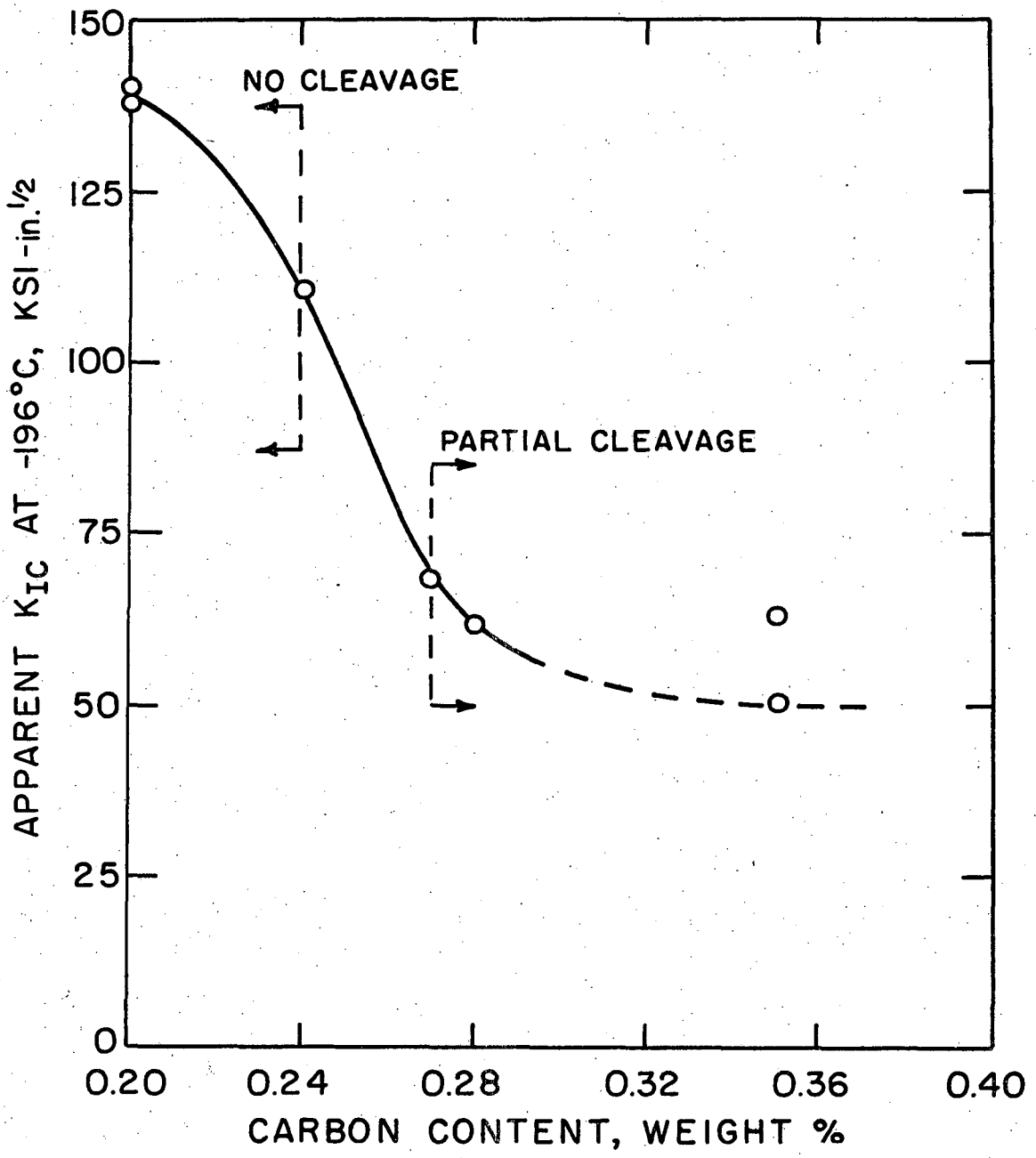

XBL 701-210

Fig. 8

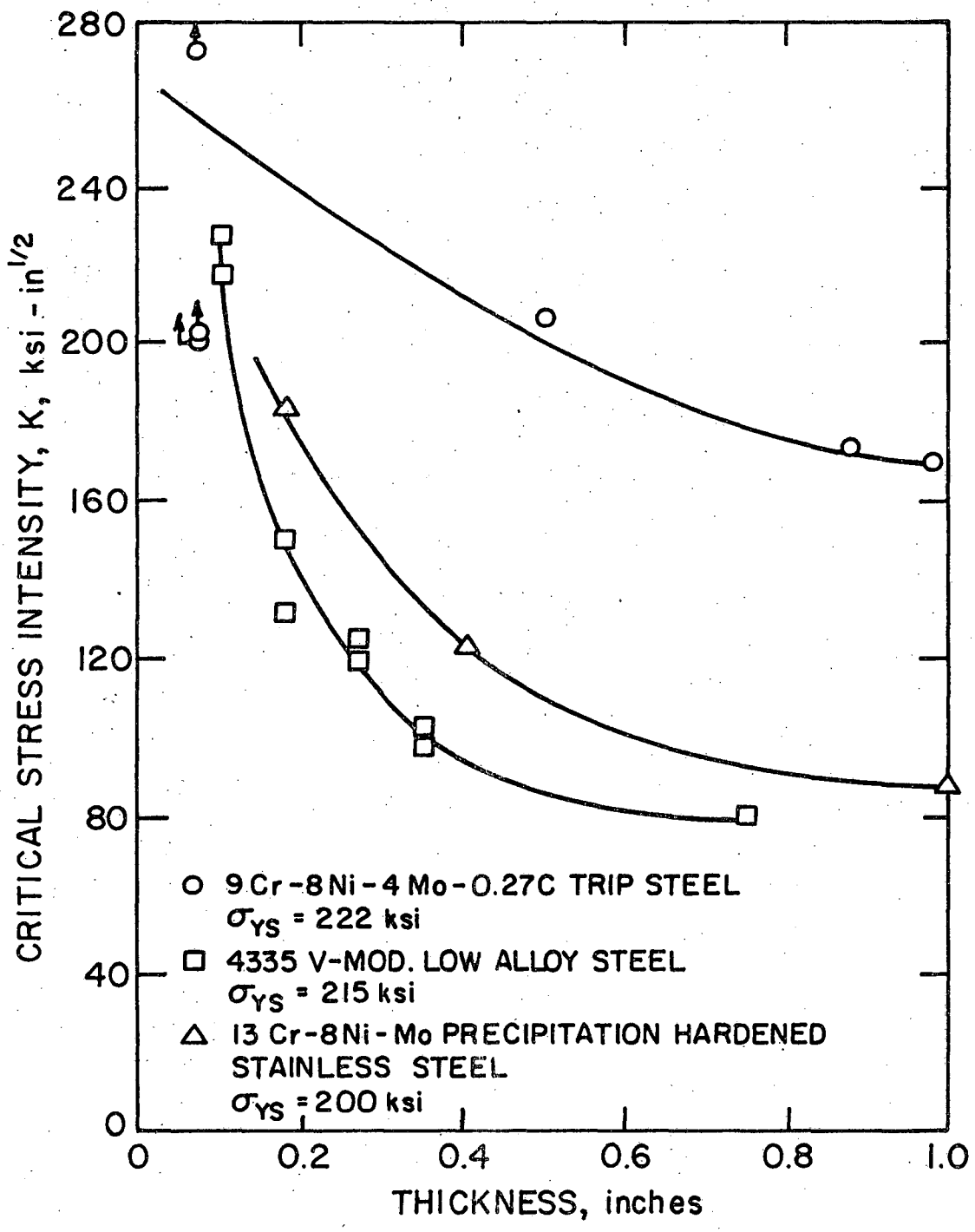

XBL6811-6156A

Fig. 9

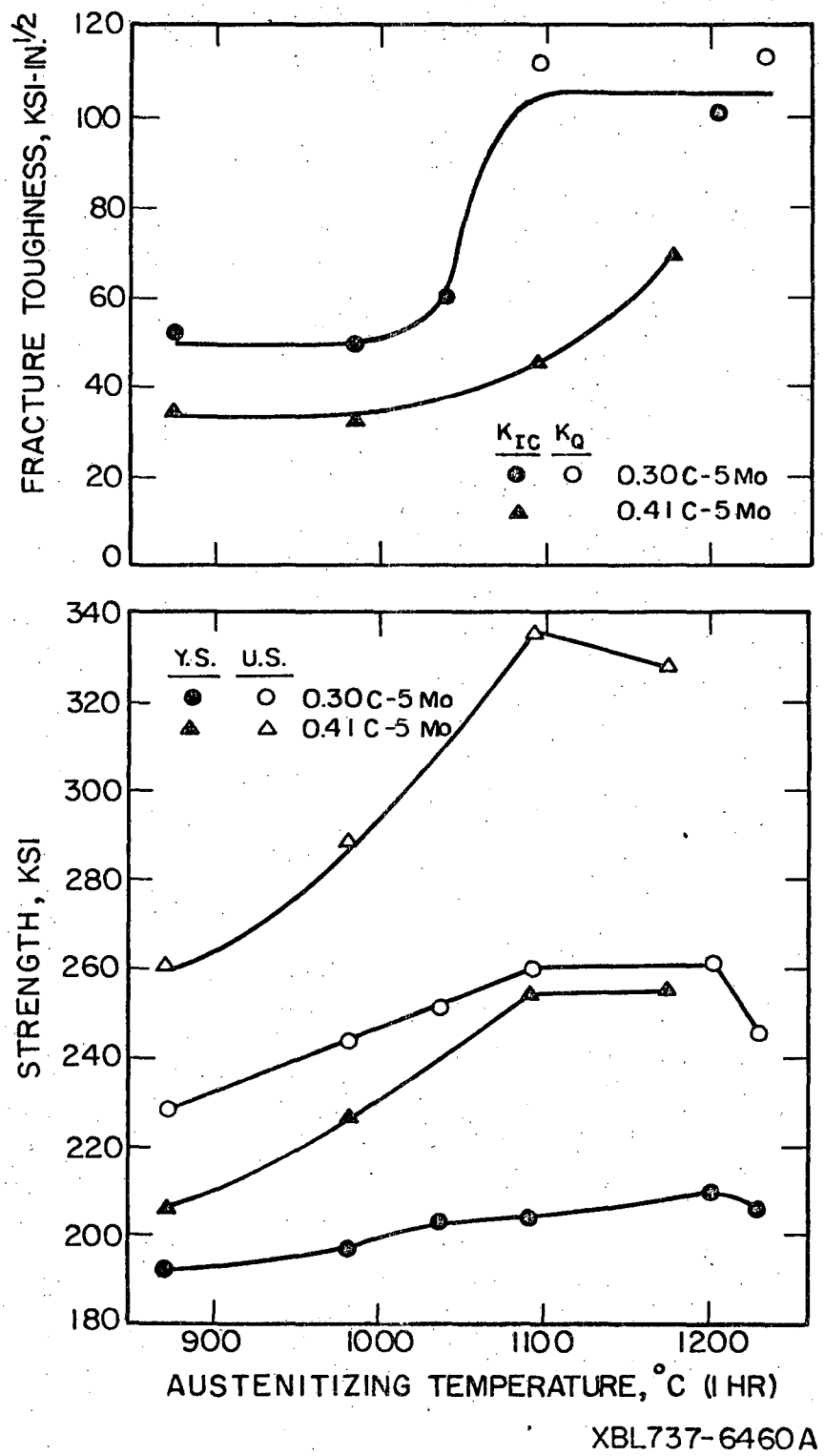
FRACTURE TOUGHNESS, KSI-IN.1/2
120
100
80
60
40
20
0
KIC KQ
0.30C-5Mo
0.41C-5Mo
STRENGTH, KSI
340
320
300
280
260
240
220
200
180
Y.S. U.S.
0.30C-5Mo
0.41C-5Mo
900
1000
1100
1200
AUSTENITIZING TEMPERATURE, °C (1 HR)
XBL737-6460A

Fig. 10

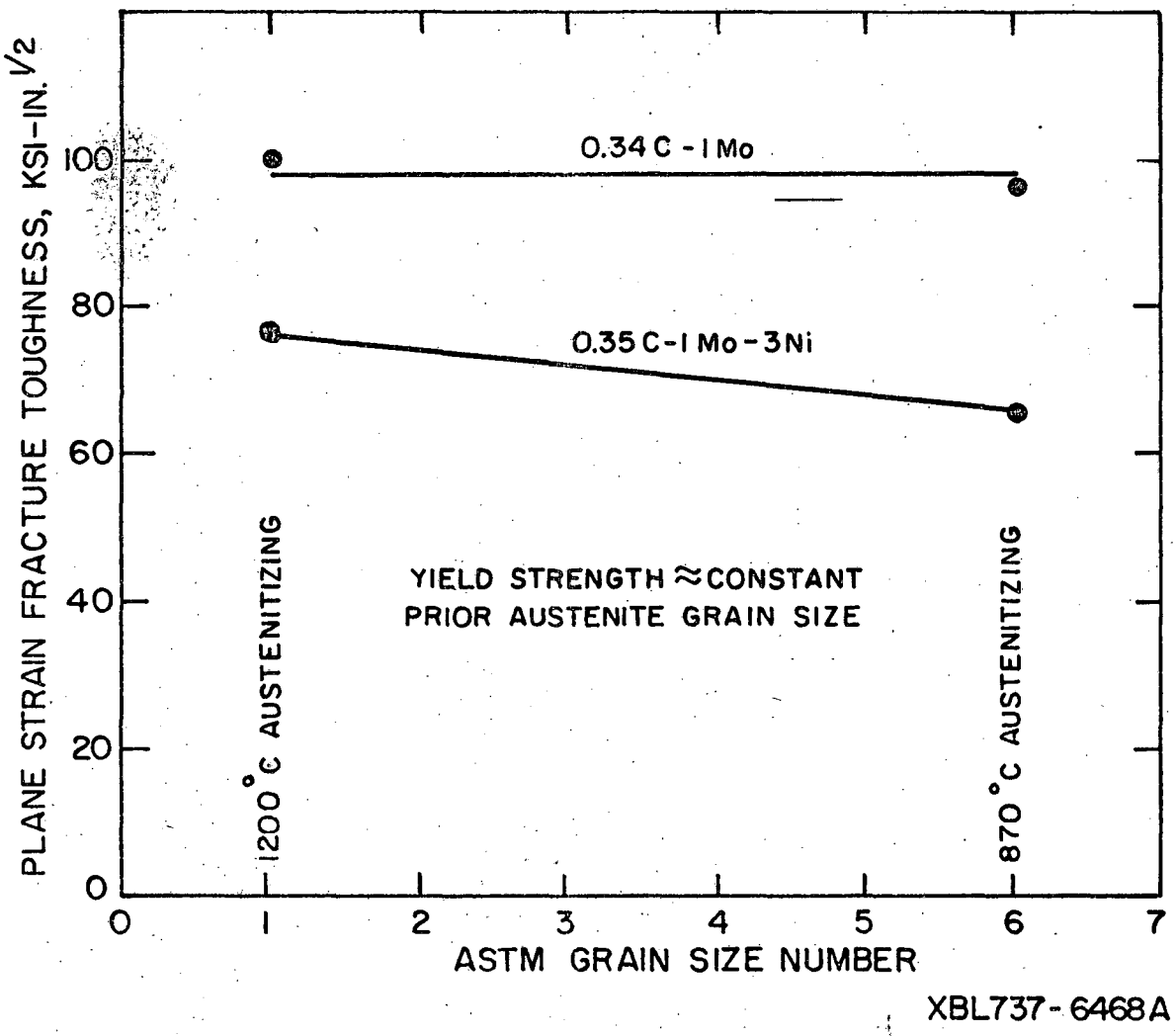
PLANE STRAIN FRACTURE TOUGHNESS, KSI-IN.$^{1/2}$
100
80
60
40
20
0
0.34 C - 1 Mo
0.35 C-1 Mo-3Ni
YIELD STRENGTH ≈ CONSTANT
PRIOR AUSTENITE GRAIN SIZE
1200 °C AUSTENITIZING
870 °C AUSTENITIZING
0
1
2
3
4
5
6
7
ASTM GRAIN SIZE NUMBER
XBL737-6468A

Fig. 11

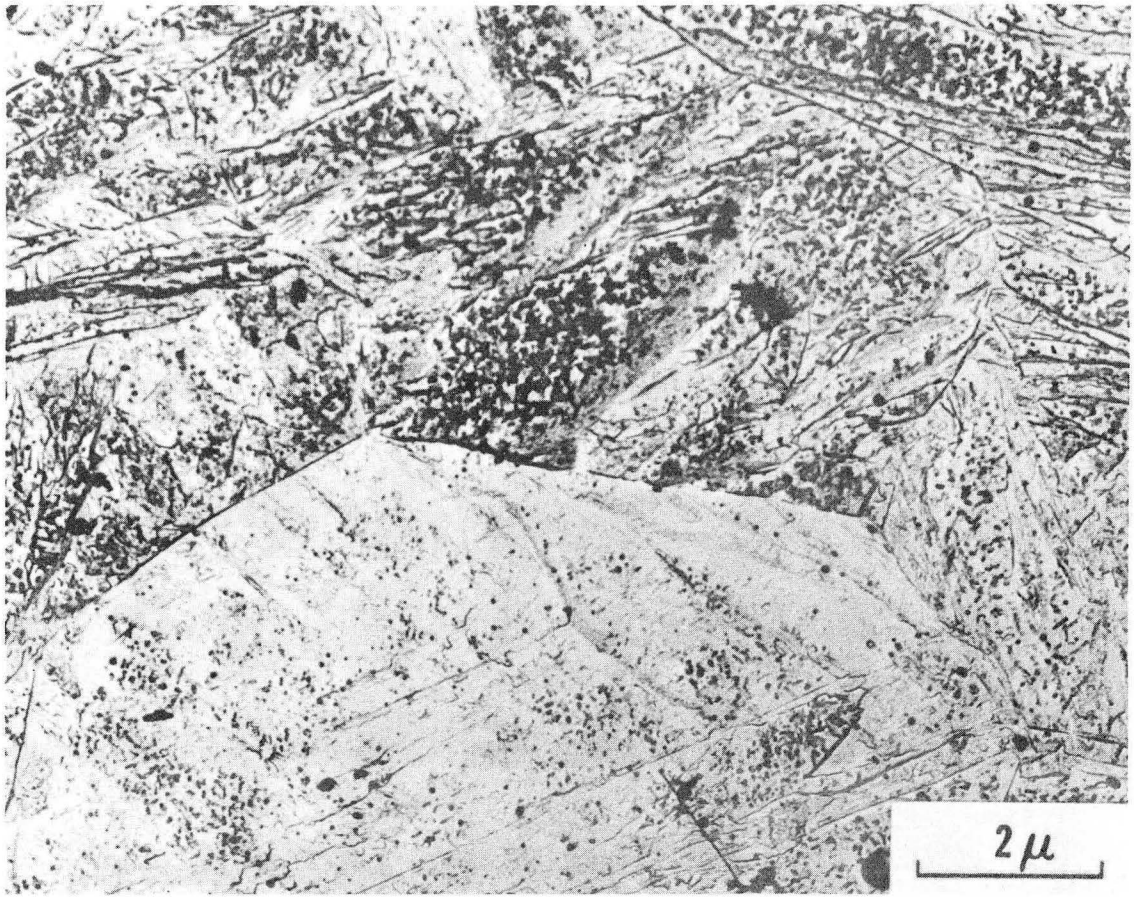

XBB 737-4410

Fig. 12

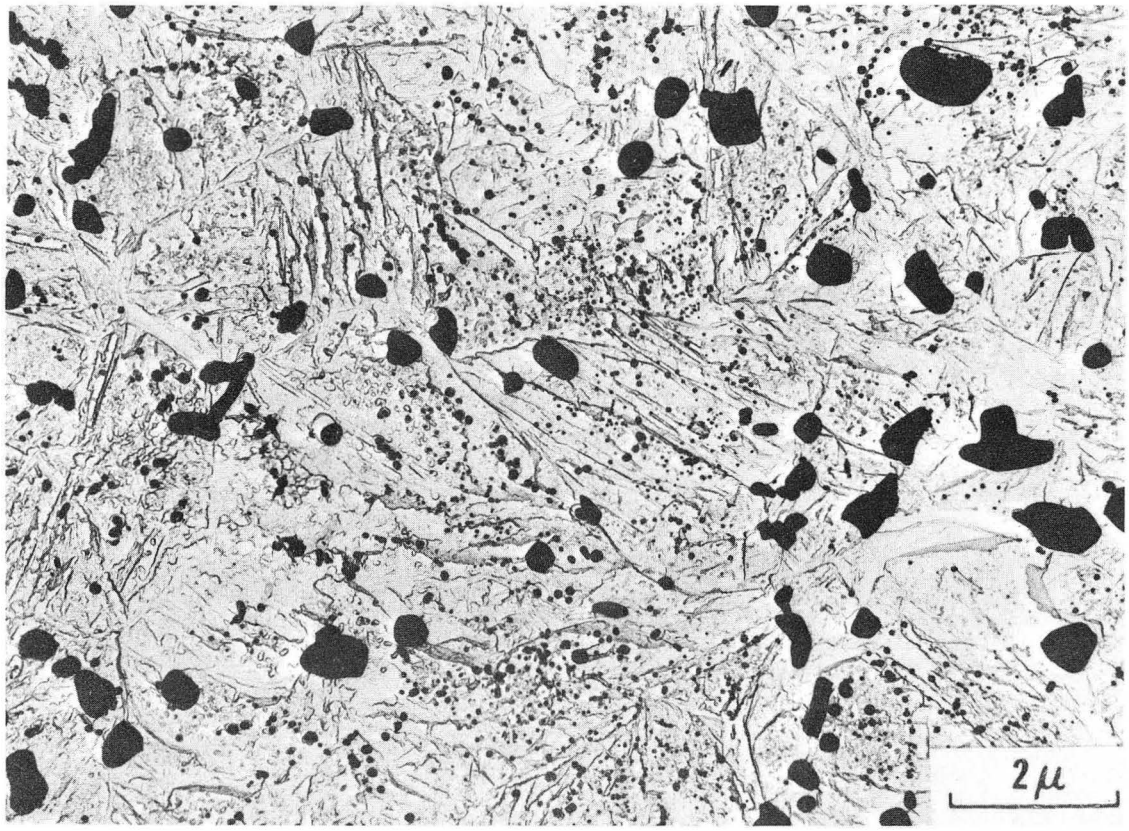

XBB 737-4407

Fig. 13

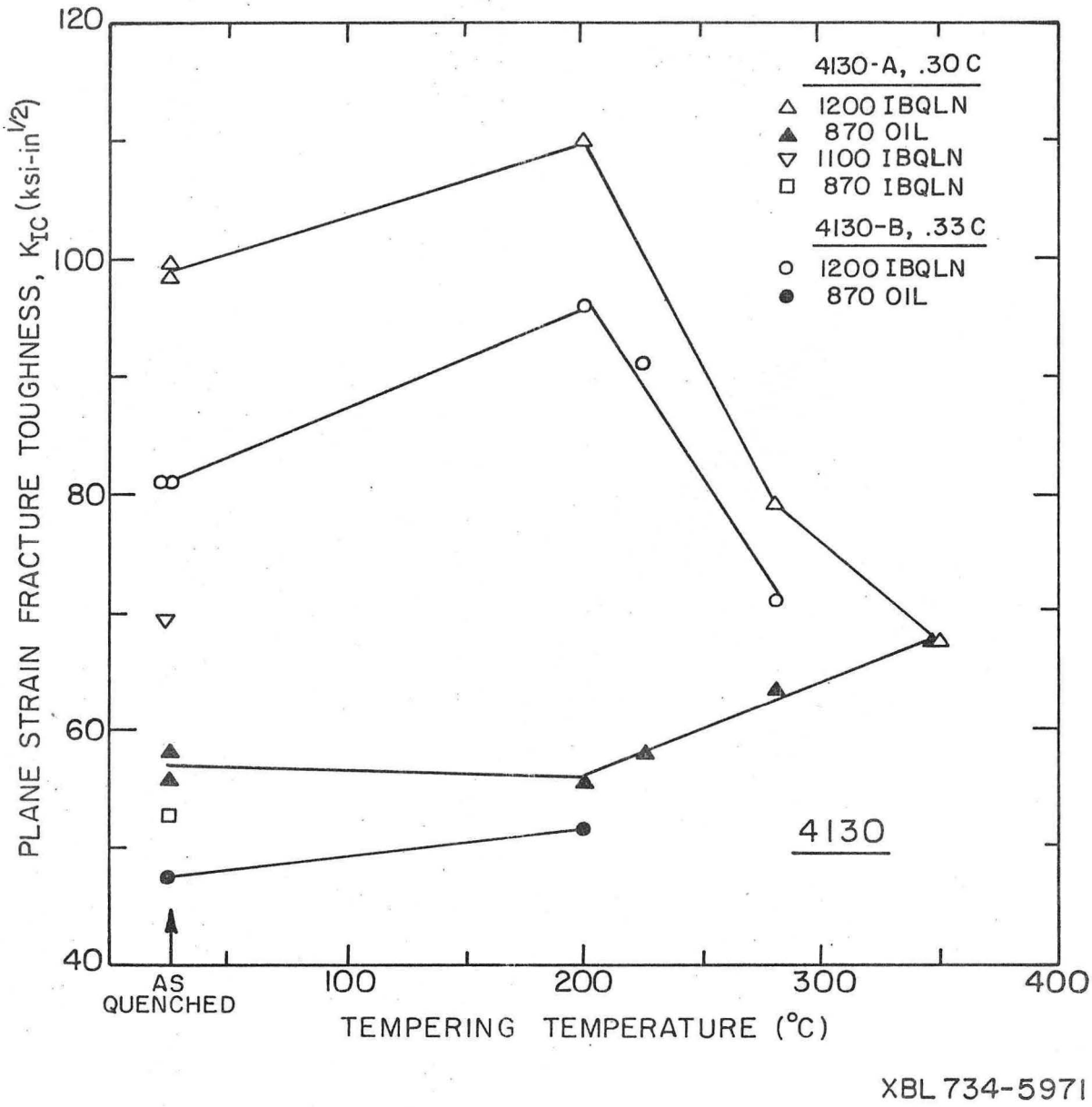

XBL 734-5971

Fig. 14

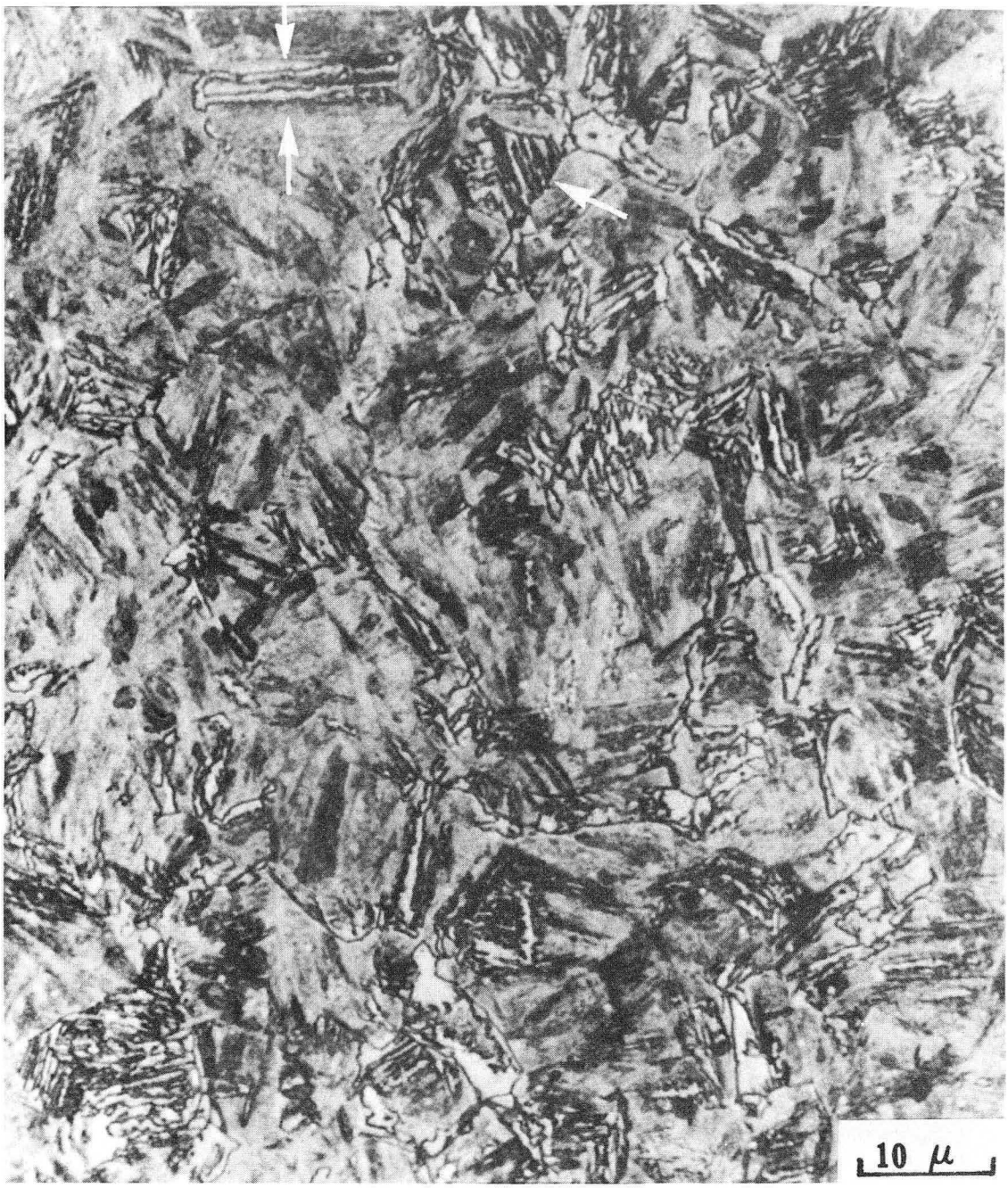

XBB 732-658

Fig. 15(a)

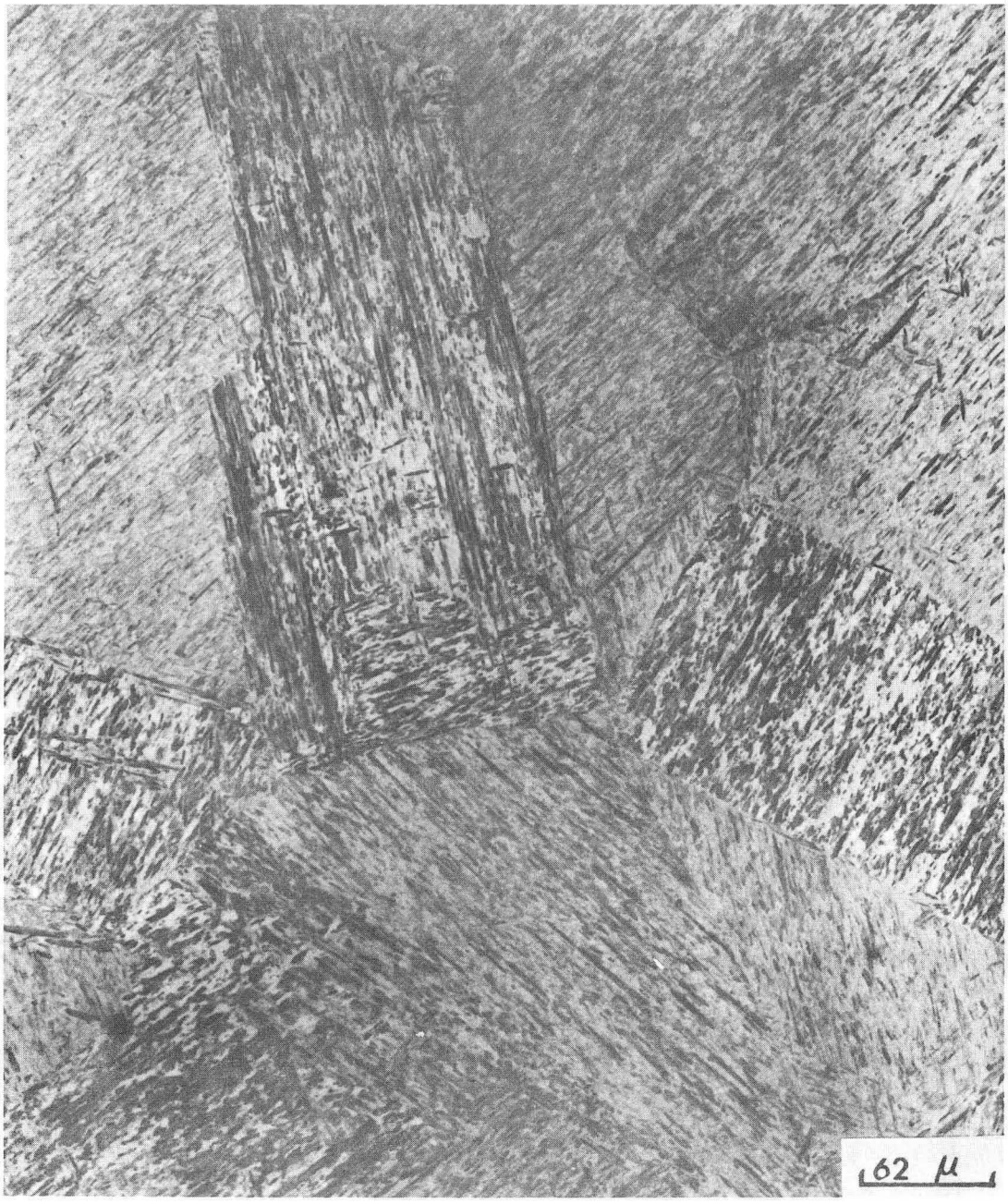

XBB 732-620

Fig. 15(b)

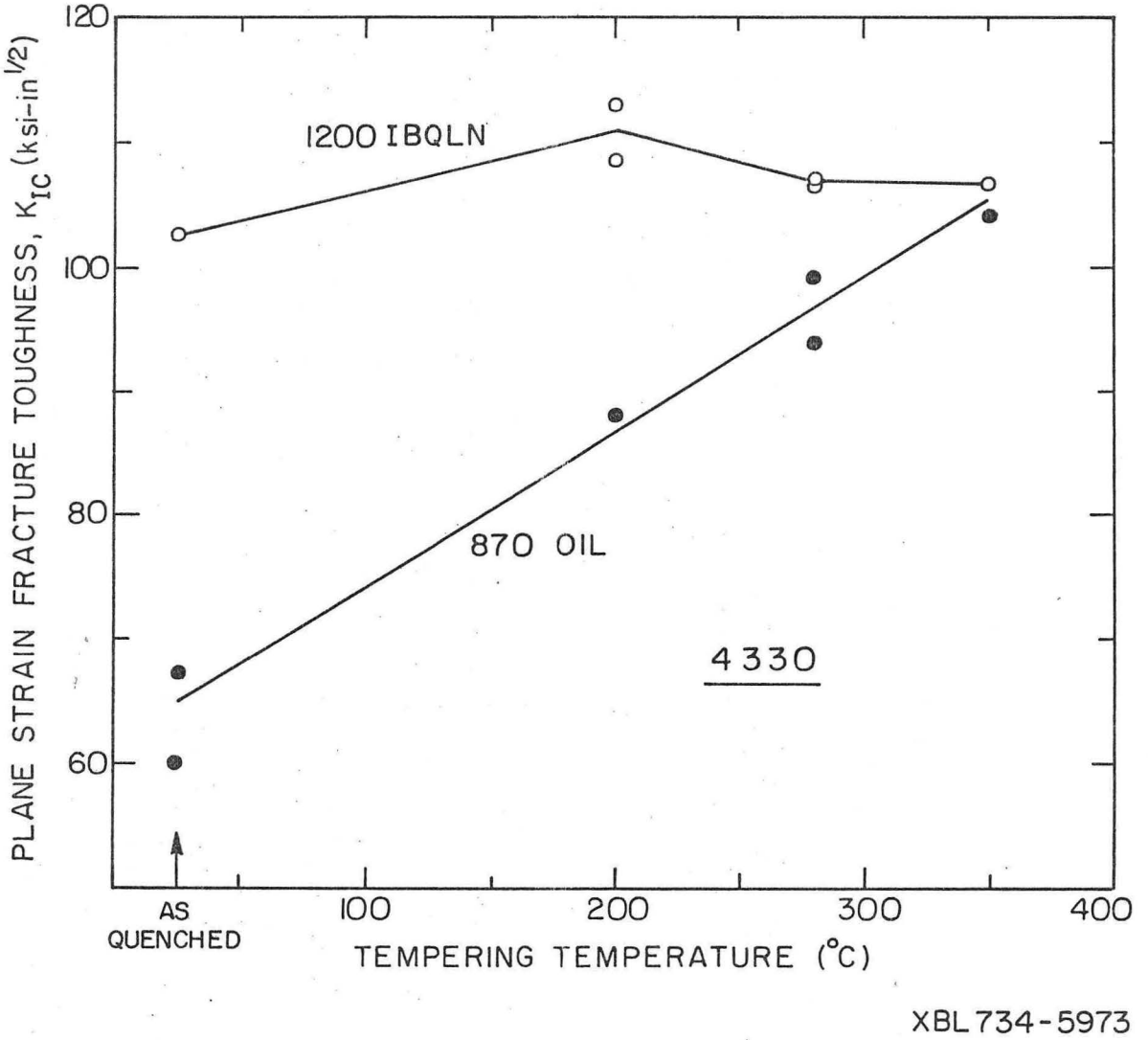
120
100
80
60
PLANE STRAIN FRACTURE TOUGHNESS, K_{IC} (ksi-in$^{1/2}$)
1200 IBQLN
870 OIL
4330
AS QUENCHED
100
200
300
400
TEMPERING TEMPERATURE (°C)
XBL 734-5973

Fig. 16

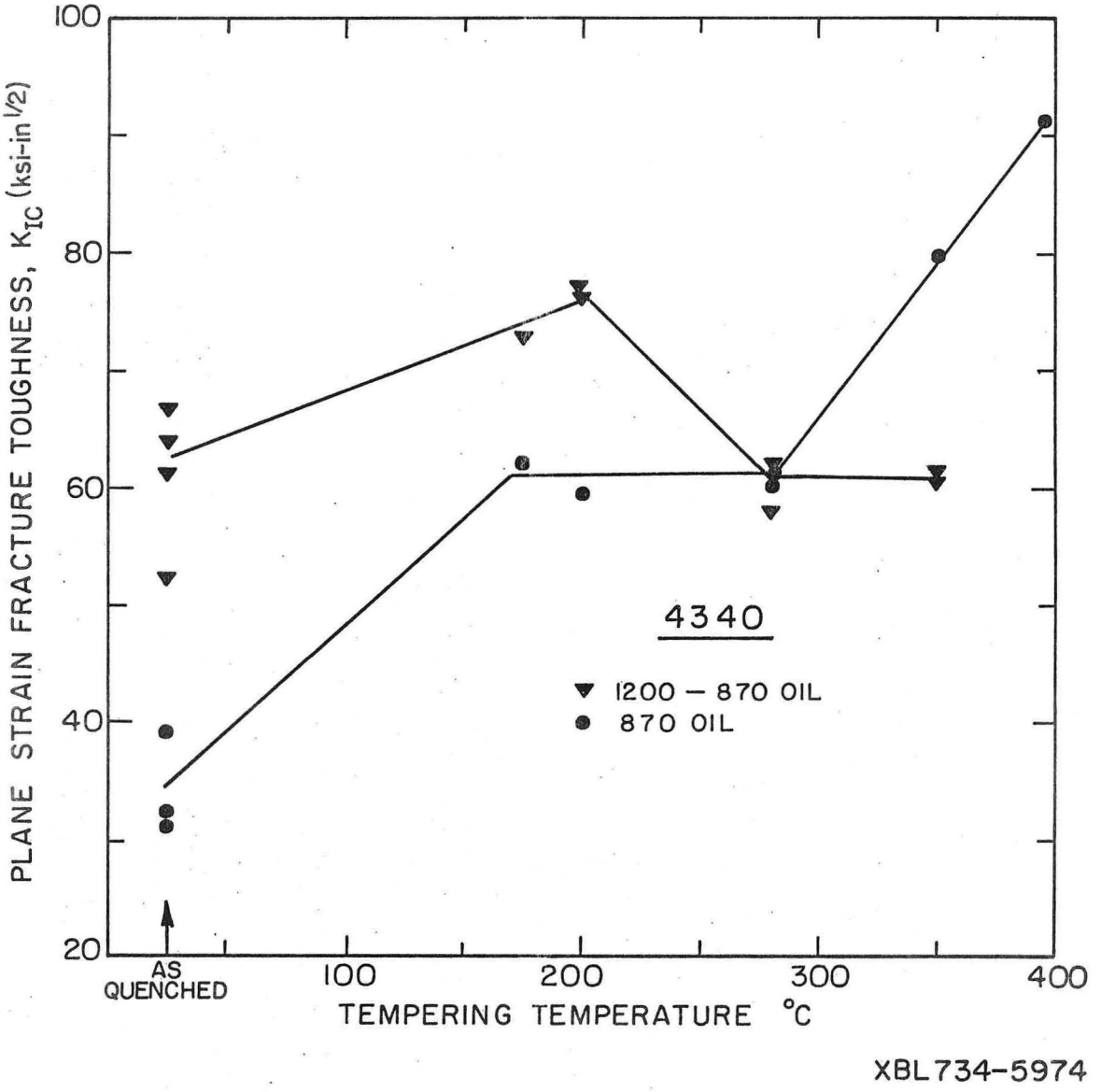
100
80
60
40
20
PLANE STRAIN FRACTURE TOUGHNESS, K_{IC} (ksi-in$^{1/2}$)
AS QUENCHED
100
200
300
400
TEMPERING TEMPERATURE °C
4340
1200 – 870 OIL
870 OIL
XBL734-5974

Fig. 17

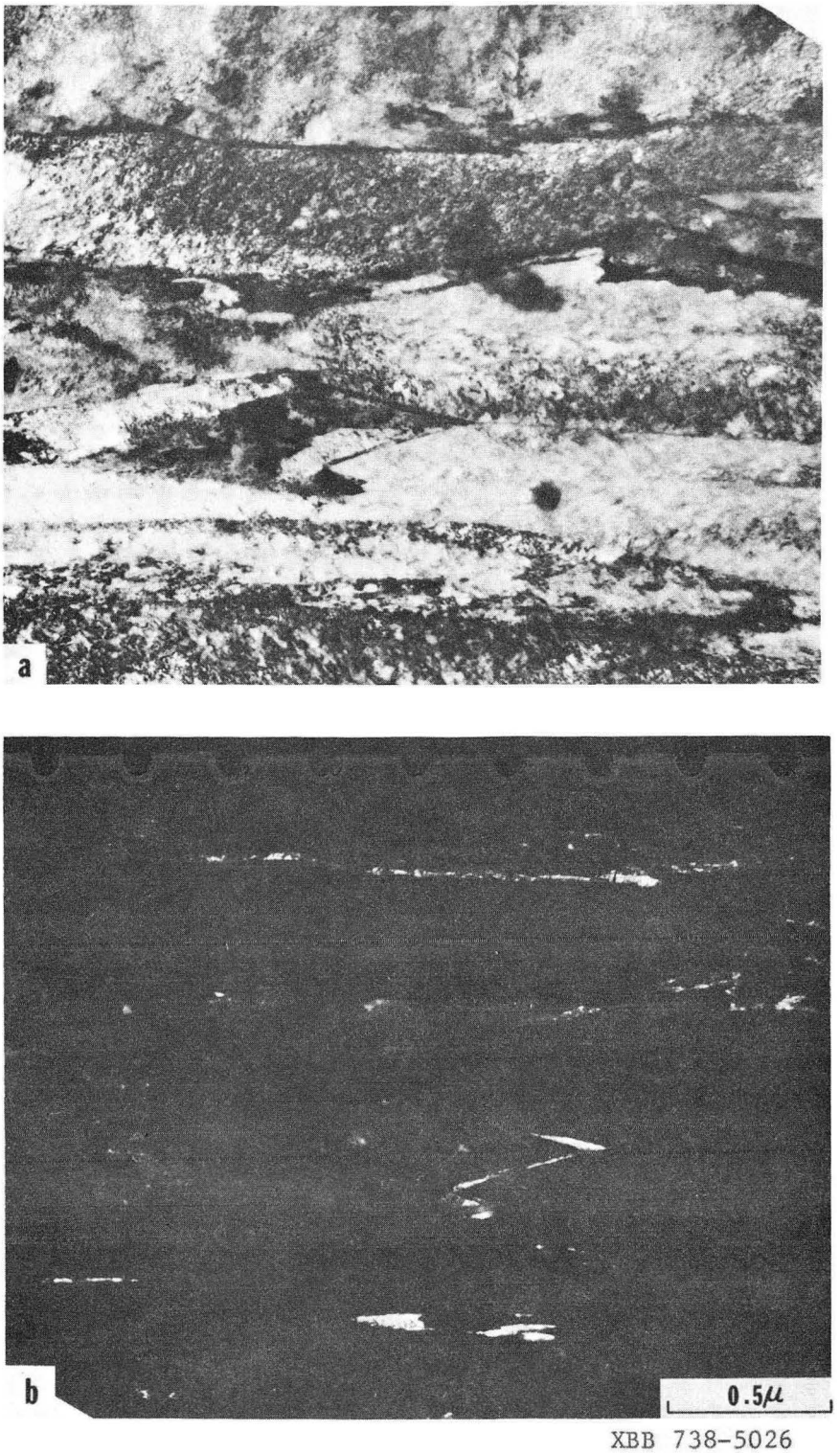

XBB 738-5026

Fig. 18

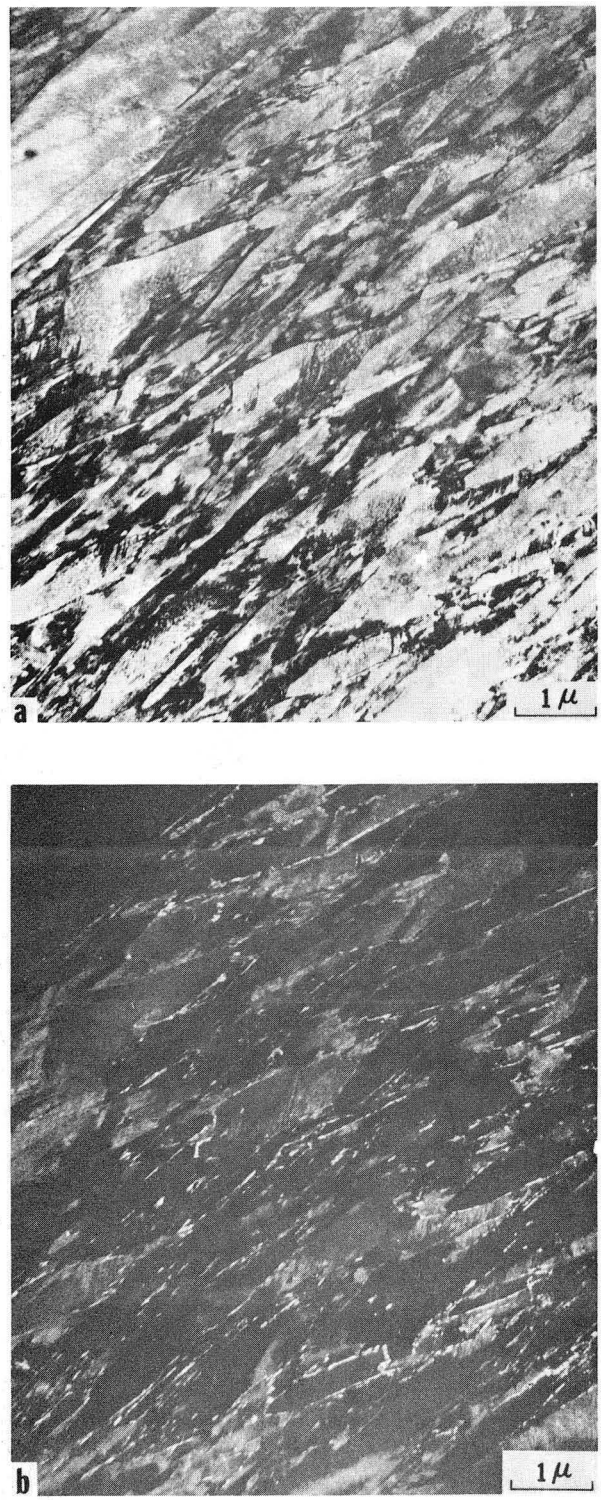

XBB 738-5025

Fig. 19

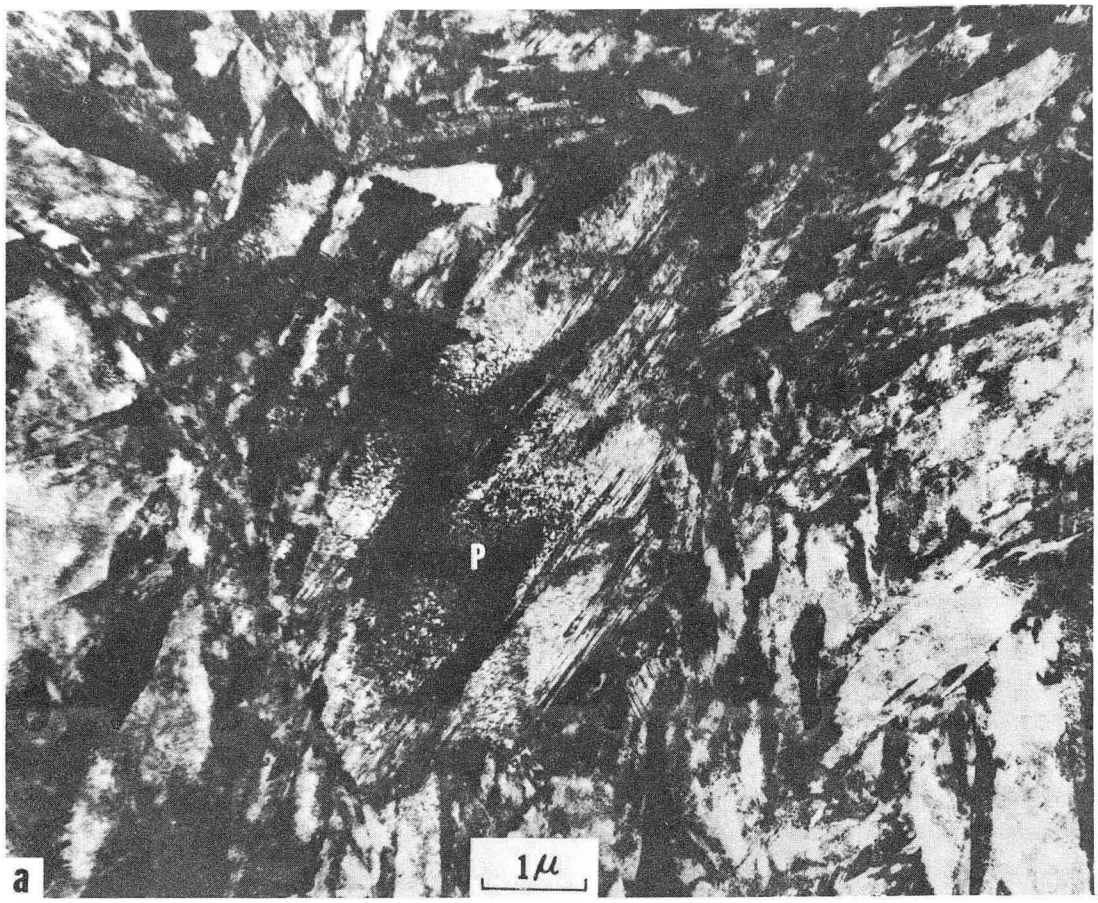

XBB 738-5018

Fig. 20(a)

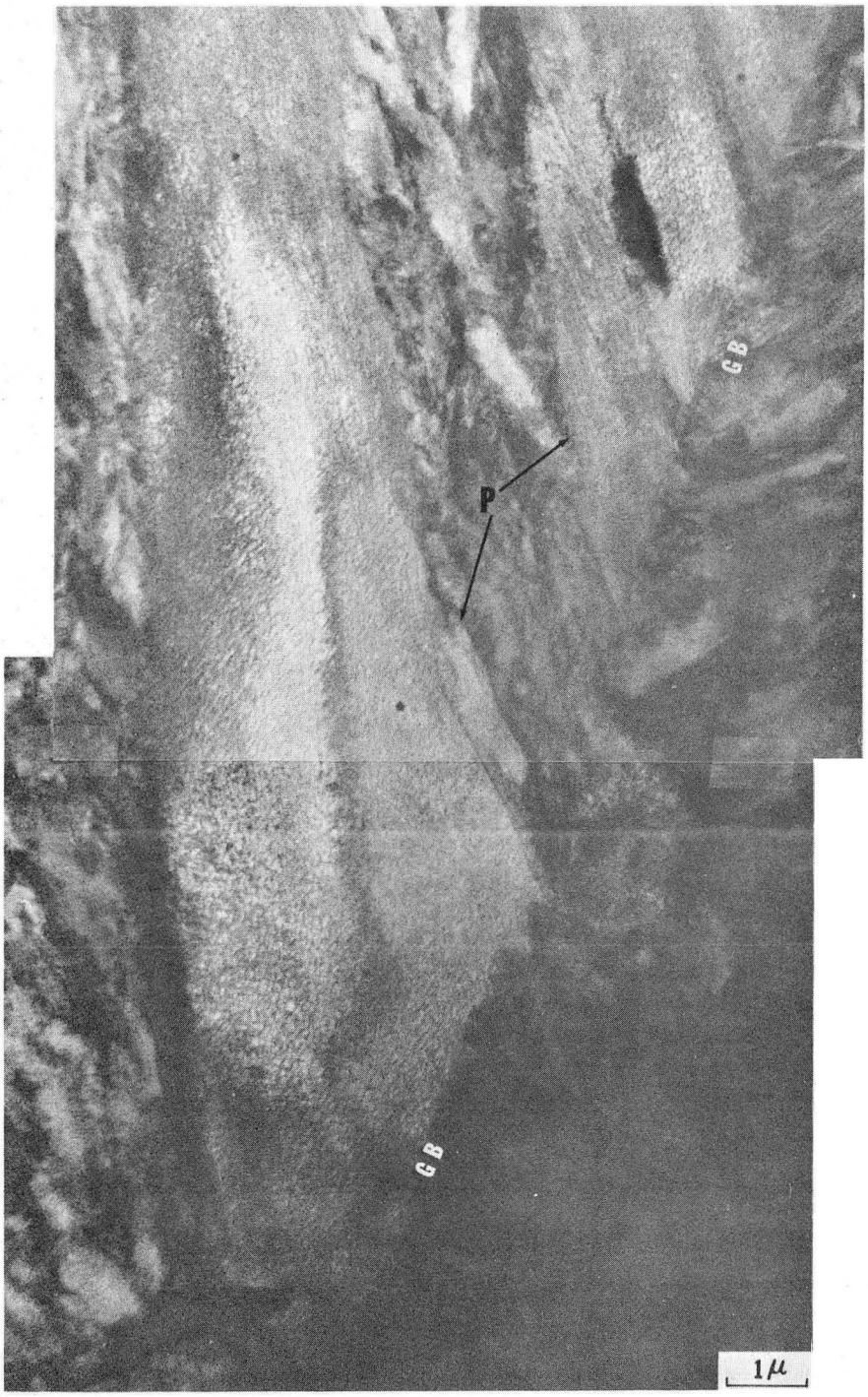

XBB 738-5028

Fig. 20(b)

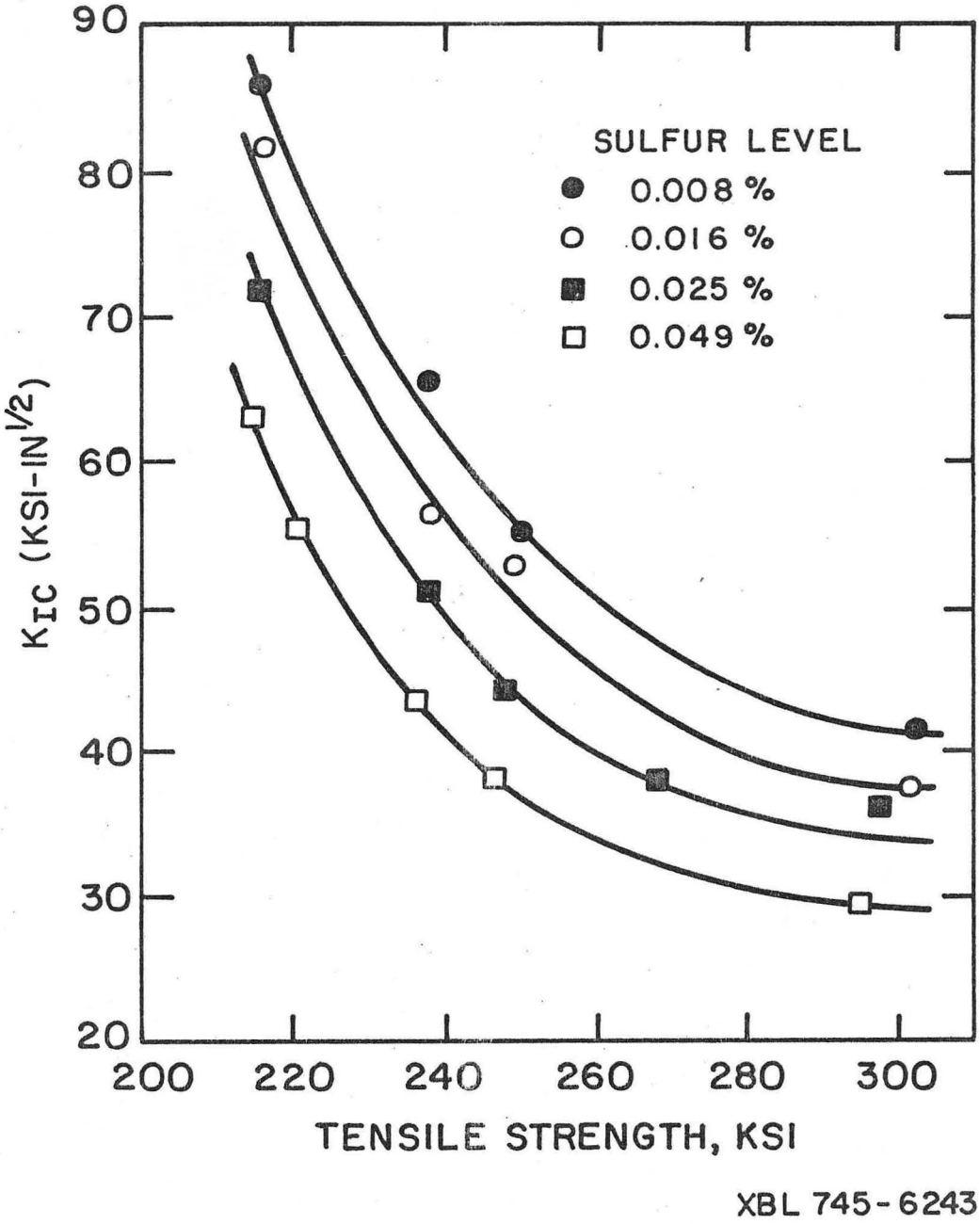

XBL 745-6243

Fig. 21

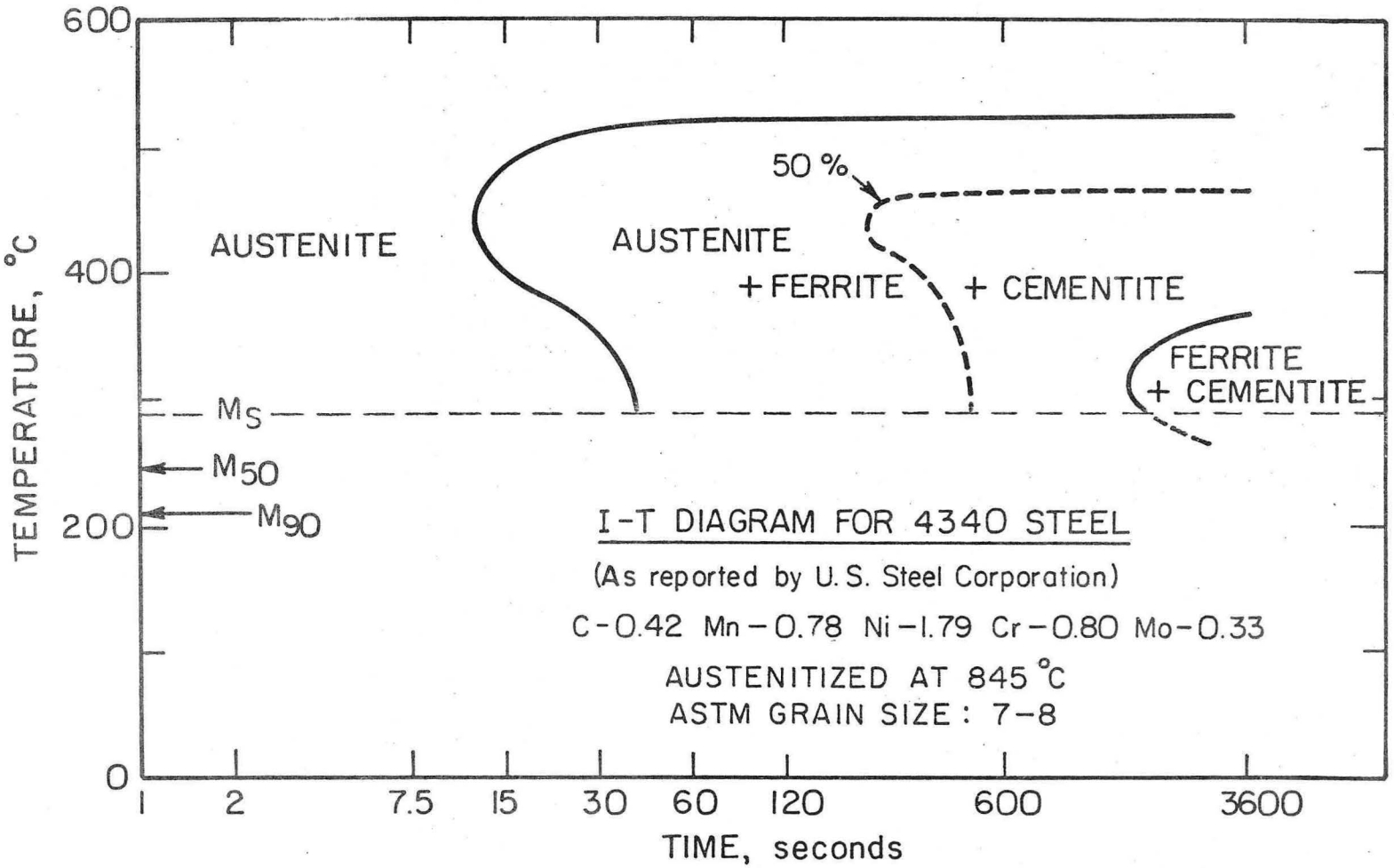

XBL 745-6289

Fig. 22(a)

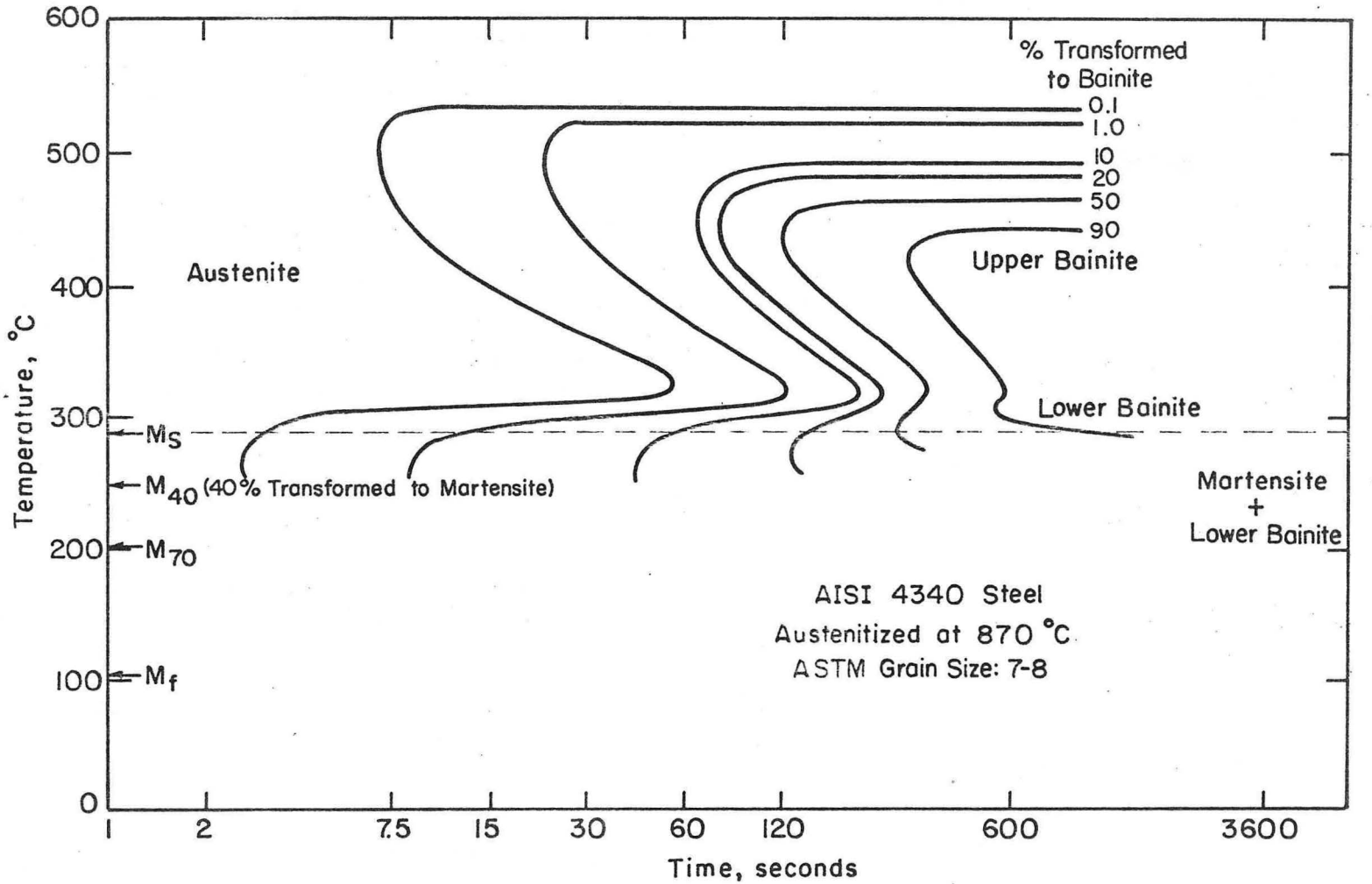

XBL7311-6666

Fig. 22(b)

LEGAL NOTICE

This report was prepared as an account of work sponsored by the United States Government. Neither the United States nor the United States Atomic Energy Commission, nor any of their employees, nor any of their contractors, subcontractors, or their employees, makes any warranty, express or implied, or assumes any legal liability or responsibility for the accuracy, completeness or usefulness of any information, apparatus, product or process disclosed, or represents that its use would not infringe privately owned rights.

TECHNICAL INFORMATION DIVISION
LAWRENCE BERKELEY LABORATORY
UNIVERSITY OF CALIFORNIA
BERKELEY, CALIFORNIA 94720